

Manuscript Number:

Title: Agglutination of benthic foraminifera in relation to mesoscale bathymetric features in the abyssal NE Atlantic (Porcupine Abyssal Plain)

Article Type: Research Paper

Keywords: abyssal hills; benthic foraminifera; elemental composition; morphometry; particle size

Corresponding Author: Mr. Paris Vasileios Stefanoudis, MSc

Corresponding Author's Institution: University of Southampton

First Author: Paris Vasileios Stefanoudis, MSc

Order of Authors: Paris Vasileios Stefanoudis, MSc; Ralf Schiebel, PhD; Romain Mallet; Jennifer M Durden, MSc; Brian J Bett, PhD; Andrew J Gooday, PhD

Abstract: Abyssal hills, small topographic features rising above the abyssal seafloor (<1000 m altitude), have distinct environmental characteristics compared to abyssal plains, notably the presence of coarser-grained sediments. As a result, they are a major source of habitat heterogeneity in the deep sea. The aim of this study was to investigate whether there is a link between abyssal hills and the test characteristics of selected agglutinated benthic foraminiferal species. We analysed 1) the overall morphometry, and 2) the granulometric and chemical (elemental) characteristics of the agglutinated tests of ten common foraminiferal species (*Adercotryma glomeratum*, *Ammobaculites agglutinans*, *Cribrostomoides subglobosum*, *Cribrostomoides* sp. 1, *Lagenammina* sp.1, four *Reophax* sp. and one indeterminate species) at four sites (two on top of abyssal hills and two on the adjacent plain) in the area of the Porcupine Abyssal Plain Sustained Observatory, northeast Atlantic. The foraminiferal test data were compared with the particle size distribution and elemental composition of sediments from the study sites in order to explore possible grain size and mineral selectivity. We found differences in the visual appearance of the tests (i.e. the degree of irregularity in their shape), which was confirmed by morphometric analyses, related to seafloor topography. The agglutinated foraminifera selected different sized particles on hills and plains, reflecting the distinct granulometric characteristics of these settings. These characteristics (incorporation of coarse particles, test morphometry) could provide evidence for the recognition of ancient abyssal hill environments, as well as other palaeoceanographic settings that were characterised by enhanced current flow. Furthermore, analyses of sediment samples from the hill and plain sites using wavelength-dispersive X-ray fluorescence (WD-XRF) yielded different elemental profiles from the plains, probably a result of winnowing on the hills, although all samples were carbonate-rich. In contrast, the majority of the agglutinated tests were rich in silica, suggesting a preferential selection for quartz.

**ABSTRACT**

Abyssal hills, small topographic features rising above the abyssal seafloor (<1000 m altitude), have distinct environmental characteristics compared to abyssal plains, notably the presence of coarser-grained sediments. As a result, they are a major source of habitat heterogeneity in the deep sea. The aim of this study was to investigate whether there is a link between abyssal hills and the test characteristics of selected agglutinated benthic foraminiferal species. We analysed 1) the overall morphometry, and 2) the granulometric and chemical (elemental) characteristics of the agglutinated tests of ten common foraminiferal species (*Adercotryma glomeratum*, *Ammobaculites agglutinans*, *Cribrostomoides subglobosum*, *Cribrostomoides* sp. 1, *Lagenammia* sp.1, four *Reophax* sp. and one indeterminate species) at four sites (two on top of abyssal hills and two on the adjacent plain) in the area of the Porcupine Abyssal Plain Sustained Observatory, northeast Atlantic. The foraminiferal test data were compared with the particle size distribution and elemental composition of sediments from the study sites in order to explore possible grain size and mineral selectivity. We found differences in the visual appearance of the tests (i.e. the degree of irregularity in their shape), which was confirmed by morphometric analyses, related to seafloor topography. The agglutinated foraminifera selected different sized particles on hills and plains, reflecting the distinct granulometric characteristics of these settings. These characteristics (incorporation of coarse particles, test morphometry) could provide evidence for the recognition of ancient abyssal hill environments, as well as other palaeoceanographic settings that were characterised by enhanced current flow. Furthermore, analyses of sediment samples from the

hill and plain sites using wavelength-dispersive X-ray fluorescence (WD-XRF) yielded different elemental profiles from the plains, probably a result of winnowing on the hills, although all samples were carbonate-rich. In contrast, the majority of the agglutinated tests were rich in silica, suggesting a preferential selection for quartz.

**KEYWORDS:** *abyssal hills, benthic foraminifera, elemental composition, morphometry, particle size.*

### Highlights

- Agglutination patterns of benthic foraminifera from abyssal hills were compared with those on the plain
- Foraminifera selected different sized particles on hills and plains, mirroring the distinct sedimentary profiles of the two settings
- Differences in the visual appearance of the tests related to seafloor topography was confirmed by morphometric analyses
- Elemental composition of the tests was similar for all studied specimens
- In contrast abyssal hills had different elemental characteristics from the plain
- Agglutinated benthic foraminifera could be used as proxy for paleoflow dynamics

# **Agglutination of benthic foraminifera in relation to mesoscale bathymetric features in the abyssal NE Atlantic (Porcupine Abyssal Plain)**

PARIS V. STEFANOUDIS<sup>1,\*</sup>, RALF SCHIEBEL<sup>2</sup>, ROMAIN MALLET<sup>3</sup>, JENNIFER M. DURDEN<sup>1</sup>, BRIAN J. BETT<sup>4</sup> & ANDREW J. GOODAY<sup>4</sup>

<sup>1</sup>Ocean and Earth Science, National Oceanography Centre Southampton, University of Southampton Waterfront Campus, European Way, Southampton SO14 3ZH, United Kingdom

<sup>2</sup>LUNAM Université, Université d'Angers, UMR-CNRS 6112, LPGN-BIAF, Laboratoire des Bio-Indicateurs Actuels et Fossiles, 2 Boulevard Lavoisier, 49045 Angers CEDEX 01, France

<sup>3</sup>SCIAM, Service Commun d'Imagerie et Analyses Microscopiques, IRIS-IBS Institut de Biologie en Santé, CHU d'Angers, LUNAM Université, 49933 Angers Cedex, France

<sup>4</sup>National Oceanography Centre, University of Southampton Waterfront Campus, European Way, Southampton SO14 3ZH, United Kingdom

\*Corresponding author (e-mail: [p.v.stefanoudis@soton.ac.uk](mailto:p.v.stefanoudis@soton.ac.uk))

## 1 1. INTRODUCTION

2 Abyssal plains are vast areas of the ocean floor situated at water depths between  
3 3500 and 6500 m. They make up almost two-thirds of the Earth's surface (Watling *et*  
4 *al.*, 2013), yet despite their immense size they have received disproportionately little  
5 scientific attention compared to other ocean habitats (Stuart *et al.*, 2008). Often  
6 regarded as topographically homogeneous, abyssal plains are populated by abyssal  
7 hills, typically up to a few hundred meters in height and a few kilometres in width.  
8 These represent one of the most important geomorphic features in the oceans  
9 (Heezen *et al.*, 1959; Heezen & Holcombe, 1965; Goff & Arbic, 2010). Abyssal hills  
10 share many environmental characteristics with larger underwater features such as  
11 submarine knolls and seamounts (Yesson *et al.*, 2011), which led to the term  
12 seamount being applied to any topographic rise >100 m high (Pitcher *et al.*, 2007;  
13 Clark *et al.*, 2010). However, here we retain the term 'abyssal hills' for relatively low  
14 (<1000 m) topographic rises located on the abyssal seafloor, and treat them as  
15 distinct topographic entities. Abyssal hills increase habitat complexity on the seafloor  
16 and may potentially alter benthic faunal patterns and diversity (Snelgrove & Smith,  
17 2002; Rex & Etter, 2010). There is an extensive literature on the effects of habitat  
18 heterogeneity on benthic diversity patterns. Studies have focussed mainly on the  
19 finer spatial scales (centimeters to meters) represented by biogenic structures and  
20 the patchy distribution of organic matter (Gooday, 1986; Levin *et al.*, 1986; Thistle &  
21 Eckman, 1990; Hasemann & Soltwedel, 2011; Warren *et al.*, 2013) but have also  
22 addressed broader scales (mesoscale, i.e. decimeters to kilometers) by comparing  
23 assemblages from environmentally contrasting sites (Thistle, 1983; Kaminski, 1985;  
24 Gage *et al.*, 1995; Baldrighi *et al.*, 2014). However, very few studies (e.g, Durden *et*

25 *al.* 2015) have explored the impacts of abyssal hills on deep-sea communities and  
26 none has dealt with meiofaunal groups such as the foraminifera.

27 Benthic foraminifera are a successful group of largely marine testate protists  
28 within the Rhizaria (Adl *et al.*, 2012; Ruggiero *et al.*, 2015). The 'tests' (shells) of  
29 some species are preserved in marine sediments and represent important proxies in  
30 palaeoceanography. They are a major component of modern soft-bottom meio- and  
31 macro-faunal communities on abyssal plains and play an important role in ecological  
32 processes on the ocean floor (Gooday *et al.*, 1992). During the analysis of  
33 foraminiferal samples collected in the area of the Porcupine Abyssal Plain Sustained  
34 Observatory (PAP-SO; Hartman *et al.*, 2012) in the northeast Atlantic (4800 m water  
35 depth) we observed apparent differences in the agglutination patterns (size and  
36 nature of the cemented particles) and morphology of benthic foraminiferal tests  
37 obtained at sites on the tops of abyssal hills and on the adjacent abyssal plain. The  
38 overall aim of this study was to investigate whether and how environmental  
39 differences between the hills and the plain affect the construction of agglutinated  
40 benthic foraminiferal tests in this region. Specifically, we were interested in 1)  
41 whether the same species select particles of different (a) sizes and (b) composition  
42 in these two settings, and 2) the extent to which any differences in particle selection  
43 influences the test morphology. To address these questions we analysed the overall  
44 morphometry as well as the granulometric and chemical (elemental) characteristics  
45 of the agglutinated tests of selected common foraminiferal species in the PAP-SO  
46 area.

47

## 48 **2. MATERIALS AND METHODS**

### 49 **2.1 Sample collection and study site**

50 Samples were collected during RSS *James Cook* Cruise 062 (JC062, 24 July to 29  
51 August 2011; Ruhl, 2012) in the vicinity of the PAPSO area. They were obtained  
52 using a Bowers and Connelly Megacorer (Gage & Bett, 2005) equipped with core  
53 tubes (59 mm internal diameter) from two abyssal plain sites (P1, P2) and two  
54 abyssal hill sites (H1, H4) (Fig. 1; Table 1). Distances between sites were in the  
55 range of tens of kilometres. On board the ship the cores were sliced into 0.5-cm-  
56 thick layers down to 2-cm sediment depth, followed by 1-cm-thick layers from 2 to  
57 10-cm depth, and each slice fixed in 10% Borax buffered formalin. The present  
58 contribution is based on material retained on a 150- $\mu$ m sieve from the 0–1 cm  
59 sediment horizon of eight samples. Sixty-five foraminiferal specimens (23 from  
60 abyssal plain sites, and 42 from abyssal hill sites) belonging to 10 agglutinated taxa  
61 were included in the analysis (Table 1). The selection of species was based on their  
62 numerical abundance and an initial assessment of the variability in the size and  
63 nature of the agglutinated particles that constituted their tests. The species, the  
64 number of specimens of each examined, and the types of analyses employed, are  
65 detailed in Appendix A. A brief description of the species is given in the Taxonomic  
66 Appendix.

67 Durden *et al.* (2015) present data on the physical characteristics for our  
68 sampling sites. Particle size distribution (0–5 cm sediment horizon) at all sites was  
69 bimodal, with peaks at 4 and 200  $\mu$ m and a trough at 22.9  $\mu$ m. The fine sediment  
70 fraction (<23  $\mu$ m) comprised mainly coccoliths, while the coarser fraction (23–1000  
71  $\mu$ m) was dominated by foraminiferal tests, indicating sediments with high carbonate  
72 content (i.e. carbonate ooze). The coarser fraction constituted a higher proportion of  
73 the sediment on the abyssal hills, where pebbles to cobble-sized ice-rafted stones  
74 were also observed. Median seabed slope was greater and more variable at the

75 abyssal hill sites compared to the plain sites, and the slope of H4 (8.6°) was more  
 76 than double that of H1 (4.0°). Organic matter input estimated from seabed images  
 77 and expressed either as the percentage of the seafloor covered by phytodetritus or  
 78 as median detritus aggregate size, did not vary spatially in the PAP-SO area.

79

**Table 1** Locality data. N<sub>1</sub>= number of replicate samples from which foraminiferal specimens have been collected and used in this study. N<sub>2</sub>= number of specimens analysed from each site. N<sub>3</sub>= Number of sediment samples for particle size analysis. N<sub>4</sub>= Number of sediment samples for elemental analysis. For geographical position of sites consult Fig. 1.

Site	Topography	Centre Latitude (N)	Centre Longitude (W)	Water depth (m)	N <sub>1</sub>	N <sub>2</sub>	N <sub>3</sub>	N <sub>4</sub>
P3	Abyssal plain	49.083	-16.667	4,851–4,853	1	4	5	1
P4	Abyssal plain	48.877	-16.293	4,849–4,851	2	19	5	2
H1	Abyssal hill	48.978	-16.728	4,669–4,679	3	16	5	1
H4	Abyssal hill	49.074	-16.243	4,339–4,388	2	26	2	1

80

## 81 **2.2 Test morphometry**

82 Initially, all 65 specimens were photographed under an incident light microscope  
 83 (Leica Z16-APO). The majority (56) were then examined by scanning electron  
 84 microscopy (SEM) using an environmental Zeiss EVO LS10 at variable pressure.  
 85 The number of SEM images was lower than the number of light microscope images  
 86 because some delicately agglutinated species collapsed upon transfer to SEM stubs  
 87 (mostly specimens of *Reophax*. sp. 14). Subsequently, both sets of images were  
 88 processed and a total of 31 morphometric parameters were obtained using image  
 89 analysis software (analySIS version 5.0, Olympus Soft Imaging Solutions). The  
 90 resulting morphometric data from both sets of microscopic images were compared

91 for consistency. As there were no significant statistical differences, the light  
92 transmission microscopy dataset, which was based on a larger number of  
93 specimens (65 compared to 56 SEM images), was selected for further analyses of  
94 the overall test morphometry (see Appendix A). Tests incorporating long spicules  
95 (mostly belonging to *Reophax* sp. 28) were not included in the analysis as the image  
96 analysis software overestimated their surface area, lowering the total number of  
97 specimens suitable for morphometric comparisons to 60 (see Appendix A).

98         Multivariate assessment of the data was computed using PRIMER 6 (Clarke  
99 & Gorley, 2006). Euclidean distance similarity matrices were created for the  
100 morphometric data and their relation to topography was explored using Multi-  
101 dimensional Scaling (MDS) and Analysis of Similarities (ANOSIM). We first worked  
102 on the complete set of morphometric parameters before focusing on the following  
103 reduced set of four parameters that seemed to drive most variation in the data: (i)  
104 Convexity, defined as the ratio between the actual measured test area (an irregular  
105 surface) and an imaginary smooth envelope that encloses the test; (ii) Maximum to  
106 Minimum Diameter ratio; (iii) Perimeter to Area ratio; and (iv) Sphericity, which gives  
107 information about the roundness of the test. In general, specimens with more  
108 irregular, “bumpier” morphologies will tend to have lower convexity and sphericity  
109 values, and higher perimeter to area and maximum to minimum diameter ratios,  
110 while the opposite will hold true for specimens with smooth surfaces and a more  
111 circular appearance. We assessed the effect of individual parameters using the  
112 Student’s t and Mann-Whitney U tests, for normally and non-normally distributed  
113 data respectively (Shapiro-Wilk test;  $p < 0.05$ ).

114         The relationship of these parameters to topography was assessed using  
115 morphometric data from all species as well as focusing on four species

116 (*Adercotryma glomeratum*, *Lagenammia* sp.1, *Reophax* sp.14 and *R.* sp. 21) that  
117 were represented by enough specimens ( $\geq 3$ ) in both settings to permit statistical  
118 comparisons (see Appendix A).

119

### 120 **2.3 Particle size**

121 Test particle size was measured from a set of 56 SEM images. Initially, an  
122 automated counting procedure was used, similar to the one described in du Châtelet  
123 *et al.* (2013a). However, it could not cope well with the heterogeneous nature of the  
124 particles found in the foraminiferal tests and therefore its use was discontinued.  
125 Instead, measurements were made manually using ImageJ (Rasband, W.S.,  
126 ImageJ, U. S. National Institutes of Health, Bethesda, Maryland, USA,  
127 <http://imagej.nih.gov/ij/>, 1997-2014), and restricted to particles  $\geq 10$   $\mu\text{m}$ . Size was  
128 determined as the longest axis dimension of the grains. In order to relate particle  
129 size to topography, the data were divided into 25 size classes based on the  
130 geometric mean particle diameter, spanning grain sizes from 10 to 295  $\mu\text{m}$ , and the  
131 resulting particle size distributions were compared. The effect of topography could  
132 be tested further for four species (*A. glomeratum*, *Lagenammia* sp.1, *R.* sp. 21, *R.*  
133 sp. 28) that were represented by sufficient specimens ( $\geq 3$ ) in both settings.

134 Grain size characteristics for the four study sites were assessed from  
135 seventeen samples (Fig. 1; Table 1) that were obtained using a Bowers and  
136 Connelly Megacorer equipped with multiple core tubes (59 and 100 mm internal  
137 diameter) (Gage & Bett, 2005). On board the ship the cores were sliced in three  
138 layers (0–1, 1–3, 3–5 cm) and each slice was stored in plastic bags with no  
139 preservative for later analysis. Sediment particle size distributions were measured by  
140 laser diffraction using a Malvern Mastersizer, after homogenisation (particles  $> 2$  mm

141 removed), dispersal in a 0.05% (NaPO<sub>3</sub>)<sub>6</sub> solution (Abbireddy & Clayton, 2009), and  
142 mechanical agitation. Detected particle sizes ranged from 0.01 to 2000 µm. The  
143 percentage of particles >63 µm in the sediments of each site and topographic setting  
144 was also estimated, as in deep-sea sediments it can serve as a proxy of current  
145 activity (McCave *et al.*, 1995; McCave & Hall, 2006). The present contribution is  
146 based on material from the 0–1 cm sediment horizon. In order to test for particle size  
147 selectivity by the foraminifera, we compared particle-size distribution data from the  
148 tests and the sediment samples, focusing on particles within the 10 to 295 µm range,  
149 which covers the same 25 size classes used to analyse foraminiferal grains.

150

## 151 **2.4 Elemental composition**

152 Quantitative estimates of the elemental composition of 56 benthic foraminiferal tests  
153 (see Appendix A) were carried out using an Environmental Scanning Electron  
154 Microscope (ESEM) (Zeiss EVO LS10) equipped with an Energy-Dispersive  
155 Spectroscopy (EDS) device (X-Max, Oxford Instruments).

156 The elemental composition of sediments from the hills and plains was  
157 determined by applying wavelength-dispersive X-ray fluorescence (WD-XRF)  
158 techniques to five samples, three from the plains and two from the hills (Table 1).  
159 Major elements were determined in fused beads obtained following fusion with a  
160 pure lithium borate flux in a Pt–Au vessel at c. 1100 °C. Lithium tetraborate (Fluxana,  
161 Germany) was used to dissolve the samples prior to major element determinations.  
162 Trace elements were analysed using pressed powder pellets. A Philips MAGIX-PRO  
163 automatic sequential WD X-ray fluorescence spectrometer was used to determine  
164 element concentrations. The elements were excited by means of a 4 kW Rh end-  
165 window X-ray tube. The instrument was calibrated using a wide range of

166 international geochemical reference samples; accuracy was typically within 5% of  
167 the consensus value when an international reference sample was run as an  
168 unknown. The  $2\sigma$  precision is typically 1–5%. Following conventional practice in  
169 geochemistry, the major element compositions were expressed as oxides. We then  
170 calculated the proportion of each element separately based on their atomic number  
171 in order to compare sediment elemental data with the elemental composition of the  
172 tests.

173

### 174 **3. RESULTS**

#### 175 **3.1 Visual comparison of agglutinated foraminifera tests from hill and plains**

176 The ten species used in this study are illustrated in Plates 1–3 and brief descriptions  
177 given in the Taxonomic Appendix. There were clear differences in the visual  
178 appearance of tests from topographically high and low sites. Specimens from the  
179 hills incorporated a higher number of larger particles (i.e.  $>100\ \mu\text{m}$ ) (Table 2) in their  
180 test walls, which gave them a more or less irregular ('lumpier') appearance with  
181 rougher surfaces than those from the plain sites (Pl. 1, figs 3–6; Pl. 2; Pl. 3). In  
182 certain species, notably *Reophax* sp. 21, which utilised some conspicuously large  
183 grains (up to almost  $300\ \mu\text{m}$  in size), the effect of these larger particles on the shape  
184 and appearance of the test was particularly evident (Pl. 2, figs 5–6). However, these  
185 striking differences did not hamper the recognition of species that were common to  
186 the two settings (e.g., Pl. 2, figs 7–10; Pl., figs 3–6).

187

#### 188 **3.2 Particle size analysis**

189 A summary of test particle size data for the agglutinated foraminifera is given in  
190 Table 2. In general, the average size and standard deviation of test particles was

**Table 2** Summary statistics of test particle size composition for species found in both hills and plains and all species for each setting combined.

Species	Plains				Hills			
	Mean ( $\mu\text{m}$ )	Median ( $\mu\text{m}$ )	SD	>100 $\mu\text{m}$	Mean ( $\mu\text{m}$ )	Median ( $\mu\text{m}$ )	SD	>100 $\mu\text{m}$
<i>Adercotryma glomeratum</i>	19.0	17.2	7.9	0%	25.6	18.5	18.1	0.8%
<i>Cribrostomoides subglobosum</i>	25.1	22.1	12.3	0.1%	24	19.3	22.7	1.7%
<i>Lagenamma</i> sp. 1	22.6	19.7	11.4	0.2%	28.8	21.1	21.8	1.6%
<i>Recurvoides</i> sp. 9	15.7	14.3	5.5	0.0%	24.8	19.6	16.1	0.3%
<i>Reophax</i> sp. 21	21.1	17.1	15.7	0.3%	33.6	19.3	35.9	6.3%
<i>Reophax</i> sp. 28	21.7	18.6	13.2	0.3%	25.3	18.5	23.2	1.4%
All species	22.1	19.3	12.0	0.1%	27	19.3	23.8	2%

191

**Table 3** Mean percentages of the coarse sediment particle fraction (>63  $\mu\text{m}$ ) against the whole range of measured particles (0.01–2000  $\mu\text{m}$ ) for each of the four study sites and topographic settings.

Site	>63 $\mu\text{m}$ (%)
P3	24.8
P4	24.9
H1	38.2
H4	63

192

193 higher for hill specimens, although median values were comparable between hills  
 194 and plains. ANOSIM results showed that the overall particle size composition of the  
 195 tests (i.e. taking into account all 25 particle size classes) was not related ( $p>0.05$ ) to

196 the topographic setting. At the species level, only *A. glomeratum* showed significant  
197 differences in particle size (ANOSIM,  $p=0.048$ ), with abyssal hill specimens utilising  
198 coarser particles on average (Table 2).

199 Sediment particle size distributions for the four studied sites were bimodal  
200 with peaks at approximately 4  $\mu\text{m}$  and 200  $\mu\text{m}$  (Fig. 2a), although on average the  
201 abyssal hills had a greater proportion of coarser material ( $>63 \mu\text{m}$ ) compared to the  
202 plain sites (Student's  $t$ ,  $p<0.05$ ) (Fig. 2a; Table 3). Within the 10–295  $\mu\text{m}$  size range,  
203 which spanned the data we used to test for particle size selectivity by the  
204 foraminifera, ANOSIM found statistically significant differences ( $p<0.01$ ) in particle  
205 size composition between hill and plain sediments.

206 An MDS ordination based on the particle size data derived from all ten  
207 species (56 specimens) and four sites (17 sediment samples) revealed differences  
208 between test and sediment samples (Fig. 2b). On an MDS plot the distance between  
209 two points corresponds to their degree of similarity in composition (i.e. closely  
210 spaced points are compositionally similar). Box-Whisker plots of the MDS x and y-  
211 ordinates against topography indicated that foraminiferal tests from the two hills  
212 contained particles that spanned a wider size range than those from the plain (Fig.  
213 2c), reflecting the greater abundance of coarse particles available in these settings.  
214 Consistent with the above-mentioned ANOSIM results, hill and plain specimens did  
215 not form well-defined groupings and had significant overlap (Fig. 2b). Sediment  
216 samples from the four sites exhibited lower levels of particle size variability  
217 compared to the tests. In the case of the plain sediments this was particularly  
218 evident from plots of the MDS x and y-ordinates against topography (Fig. 2c).

219

220

221 Sediment samples were also clearly separated from most of the tests (Fig. 2b). This  
222 was to be expected, as the sediment particle data used extends several size classes  
223 below and above the studied size range (10–295  $\mu\text{m}$ ). Consequently, sediment  
224 samples had higher proportions of coarser particles compared to the foraminifera,  
225 which always included only a few coarse grains in their tests (Fig. 2d).

226 Unlike the foraminiferal tests, hill and plain sediment samples showed no  
227 overlap on the MDS plot, further highlighting their different particle size compositions  
228 (Fig. 2b). Interestingly, H1 sediment samples were positioned between the plain (P3,  
229 P4) and the H4 samples, indicating an intermediate composition. In order to explore  
230 this further, an additional ANOSIM of sediment particle data against study site was  
231 performed. Initial results were significant ( $p < 0.01$ ), and further pairwise comparisons  
232 revealed that the particle size composition was similar between the two plain  
233 samples (P3, P4), but significantly different from the hill site H1 (P3 vs. H1,  $p = 0.016$ ;  
234 P4 vs. H1,  $p < 0.01$ ). Unfortunately, the low number of sediment samples (2) from H4  
235 did not permit pairwise comparisons with the rest of the sites, but based on their  
236 positioning on the ordination plot (Fig. 2b) we assume that the particle-size  
237 composition is different from both plain samples, and perhaps from H1 as well.

238 In the light of these findings, we wanted to explore the inconsistency between  
239 the coarser sediments at H4 and the apparent lack of correlation between test  
240 particle sizes and topographic setting. To do this we performed an additional  
241 ANOSIM on particle size data from all 56 tests against the study sites P4, H1 and H4  
242 (P3 had particle data only from two specimens and thus could not be compared).  
243 This analysis yielded significant results ( $p = 0.021$ ). Additional pairwise comparisons  
244 demonstrated that specimens from H4 had significantly different particle size

245 composition compared to specimens from P4 ( $p < 0.01$ ) as well as H1 ( $p = 0.036$ ),  
246 whereas H1 specimens were not different from P4.

247

### 248 **3.3 Morphometric analysis**

249 Multivariate analysis of morphometric data (31 parameters) did not reveal significant  
250 differences in test morphology between foraminiferal tests from abyssal hills and  
251 plains. Further analyses using a reduced set of four parameters (convexity,  
252 maximum to minimum diameter ratio, perimeter to area ratio and sphericity)  
253 produced significant results (ANOSIM,  $p < 0.01$ ), although further tests did not  
254 attribute this variation to any single morphometric character.

255 At the species level, ANOSIM with 31 morphometric parameters yielded  
256 significant differences related to topography only in the case of *Adercotryma*  
257 *glomeratum* ( $p < 0.035$ ). *Reophax*. sp. 21 showed variation in test morphology  
258 between hills and plains only when taking into account the reduced set of four  
259 parameters (ANOSIM,  $p < 0.018$ ). Furthermore, Student's t and Mann-Whitney U tests  
260 identified differences in the convexity and sphericity of *R.* sp. 14 ( $p = 0.027$  and  
261  $p = 0.048$ , respectively) as well as in the maximum to minimum diameter ratio and  
262 sphericity of *R.* sp.21 ( $p < 0.01$  in both cases).

263 All the morphometric characters estimated for the studied specimens can be  
264 found in Appendix B.

265

### 266 **3.4 Elemental analysis**

267 ESEM-EDS identified a total of 16 elements (10 major and 6 trace) from 56 benthic  
268 foraminiferal tests. Silica (Si) was by far the most abundant element, reflecting high  
269 quartz content, consistent with peaks in Si and oxygen (O) in most EDS spectra.

270 WD-XRF identified a total of 11 major elements and 21 trace elements in the five  
271 sediment samples taken from the four study sites. Ca was the dominant element,  
272 with CaO constituting approximately 39% in all samples (41% and 37% in hill and  
273 plains samples, respectively) reflecting the presence of carbonate oozes at the PAP-  
274 SO. The next most abundant element was Si, with SiO constituting approximately  
275 15% in all samples (14% and 17% in hill and plain samples, respectively).

276 The elemental composition of the foraminiferal tests was markedly different  
277 from that of the sediment samples (ANOSIM,  $p < 0.01$ ; Fig. 3a). There was no  
278 significant correlation with topographic setting for all studied material (56 tests  
279 belonging to 10 species) or for individual species (*A. glomeratum*, *Lagenammia*  
280 sp.1, *R. sp. 14* and *R. sp. 21*). This was further demonstrated by the considerable  
281 overlap of species from both settings in the MDS plot (Fig. 3b). On the other hand,  
282 MDS of the sediment elemental data yielded distinct clusters for abyssal hill and  
283 abyssal plain sites, respectively (Fig. 3c). An additional t-test on the MDS X-ordinate  
284 of the five sediment samples was significant ( $p < 0.01$ ), indicating distinct elemental  
285 profiles for abyssal hills and plains.

286 All the data used for the elemental analysis can be found in Appendix C.

287

## 288 **4. DISCUSSION**

### 289 **4.1 Limitations of dataset**

290 As our samples were fixed in formalin, we could not obtain molecular data to support  
291 our contention that the same foraminiferal species occur at the hill and plain sites.  
292 However, we took considerable care to compare specimens using light and scanning  
293 electron microscopy and are confident that similar specimens can be considered  
294 conspecific on the basis of morphological characters (see Taxonomic Appendix).

295 The particle size analysis of the agglutinated tests was based on two-  
296 dimensional SEM images in which only one side of each specimen was visible. In  
297 addition, particles <10 µm were too small to be reliably measured from SEM images  
298 and therefore this finest sediment fraction could not be included in the analysis.  
299 Creating an automated, accurate and high-resolution (sub-micron scale) method for  
300 counting the entire range of agglutinated particles in benthic foraminiferal tests  
301 remains a challenge for the future.

302

#### 303 **4.2 Do agglutinated foraminifera utilize different sized particles in hill and plain** 304 **settings?**

305 In the deep sea, areas with elevated current activity have been shown to consist of  
306 coarse-grained sediments as a result of winnowing processes (Kaminski, 1985;  
307 Schröder, 1988; Aller, 1989); these areas include topographic high points such as  
308 seamounts (Genin *et al.*, 1986; Levin & Nittrouer, 1987; Levin & Thomas, 1989).  
309 Although we lack current-meter data for our specific study sites, sediment grain-size  
310 distributions provide some indication of the hydrodynamic regime at our study sites.  
311 In the deep sea, sediments of the 10–63 µm range (sortable silt) are thought to be  
312 most easily eroded by current activity (McCave *et al.*, 1995; McCave & Hall, 2006).  
313 Thus, higher proportions of particles >63 µm should be an indicator of enhanced  
314 current flow. This has been empirically established for a large abyssal hill (height  
315 >900 m) in the PAP-SO area, where numerical modelling predictions of higher flow  
316 intensity above parts of the topographic feature correlated well with actual grain-size  
317 patterns (i.e. higher proportions of particles >63 µm) found the sedimentary record  
318 (Turnewitsch *et al.*, 2004; Turnewitsch *et al.*, 2013). The sediments on the abyssal  
319 hills that we sampled consisted, on average, of greater proportions of particles >63

320  $\mu\text{m}$  compared to the adjacent abyssal plain (Table 3). In addition, hill sites from this  
321 area (including H1 and H4), were found to have greater median seabed slope  
322 compared to plain sites (including P3 and P4) (Durden *et al.*, 2015). Considering the  
323 above, substantial hydrographic differences between our hill and plain sites (i.e.  
324 elevated current activity above the hills) are likely.

325 Our results suggest that differences in sediment granulometry between our  
326 plain and hill sites are reflected in differences in foraminiferal test agglutination.  
327 Specimens collected from abyssal hills agglutinated larger particles, mirroring the  
328 coarser nature of the surrounding sediments. This was evident simply from a visual  
329 comparison of specimens from the hill and plain settings, with the latter having a  
330 more irregular morphology than the former (Pl. 1, figs 3–6; Pl. 2; Pl. 3), although  
331 those differences were not confirmed by numerical analyses. Similarly, at the  
332 species level statistical analyses revealed no significant differences in test particle  
333 size composition with topography for the rest of the species, except in the case of *A.*  
334 *glomeratum*. This is probably because the number of large agglutinated grains ( $>100$   
335  $\mu\text{m}$ ) was low in relation to the finer-grained component. A few coarse grains  
336 incorporated in an otherwise finely agglutinated foraminiferal test can have a  
337 disproportionate effect on its overall shape and appearance (e.g. Pl. 2, figs 3–6).  
338 Another factor may be that we grouped together the two abyssal hill sites (H1 and  
339 H4), despite their significant bathymetric differences (see Table 1). H4 was located  
340 at the top of the highest and steepest hill and was characterised by a much larger  
341 fraction of particles  $>63 \mu\text{m}$  compared to H1 (Table 3). Similarly, pairwise  
342 comparisons using ANOSIM revealed that specimens from H4 had significantly  
343 coarser agglutination than those from H1. By amalgamating data from these two  
344 topographic high sites and comparing them to the plain, statistical differences in test

345 particle size composition of foraminifera became insignificant.

346         Based on visual inspection of the specimens combined with statistical tests,  
347 we conclude that the agglutinated foraminiferal species included in this study were  
348 not selecting for particular particle sizes. Instead, the composition of their tests  
349 reflected the sedimentary environment in which they resided. In some early culture  
350 experiments, Slama (1954) observed that *Ammobaculites*, a genus included in the  
351 present study (Pl. 3, figs 7–8), indiscriminately agglutinated particles of different  
352 composition and size. Since then, further studies have demonstrated non-selectivity  
353 for particle size in some agglutinated foraminifera (Buchanan & Hedley, 1960; Wells,  
354 1985; Thomsen & Rasmussen, 2008; du Châtelet *et al.*, 2013c; du Châtelet *et al.*,  
355 2013b). In a comparative study of benthic foraminiferal assemblages between two  
356 deep-sea habitats in the central north Pacific and western north Atlantic, Schröder  
357 (1986) and Schröder *et al.* (1988) found that certain species, including their *Reophax*  
358 *scorpiurus*, which resembles *R.* sp. 21 of the present study (see Taxonomic  
359 Appendix), were non-selective for particle size and thus exhibited wide  
360 morphological variability in different sedimentary environments.

361

#### 362 **4.3 Does the composition of the substratum affect test morphometry?**

363 To our knowledge, only a few studies have examined the relationship between  
364 substratum and the test morphometry of agglutinated foraminifera. Hada (1957)  
365 observed that foraminifera living in coarser sediments have coarser test surfaces.  
366 Haake (1977) noted that tests of *Textularia pseudogamen* become broader (i.e.  
367 higher width/length ratio) on coarser sediments. Schröder (1986) and Schröder *et al.*  
368 (1988) commented on the intraspecific morphological variability of *Reophax* species  
369 as a response to different substratum characteristics (see previous section). With the

370 exception of Haake (1977), the results from the rest of the studies were qualitative  
371 as they were mainly based on visual observation of the tests. Such approaches can  
372 be informative and have been successfully applied in paleoenvironmental studies  
373 (e.g. Kaminski & Schröder, 1987). However, in order to detect trends in the shape of  
374 agglutinated tests under different environmental conditions, quantitative  
375 morphometric data are necessary. The present work is the first to investigate  
376 changes in test morphology related to different sedimentary environments both  
377 qualitatively (i.e. visual observation of tests) and quantitatively (i.e. by using a range  
378 of morphometric parameters).

379 We failed to find clear evidence for differences in particle size selection  
380 between the agglutinated foraminiferal tests from the hill and plain sites, despite the  
381 different granulometric profiles of the two topographic settings. Nevertheless, all  
382 species that could be compared directly had more irregularly shaped tests at the  
383 highest site (H4) as a result of the incorporation of a relatively few large grains (Pl. 1,  
384 figs 3–6; Pl. 2; Pl. 3). This was particularly evident in the case of *Reophax* sp. 21.  
385 These obvious visual differences were confirmed by morphometric analyses. A  
386 comparison of all agglutinated tests between abyssal hill and plain sites  
387 demonstrated that there is a systematic morphometric difference that could not be  
388 expressed in terms of a single character. Instead, a combination of four parameters  
389 (convexity, maximum to minimum diameter ratio, perimeter to area ratio and  
390 sphericity) was more effective in differentiating tests from the two settings.

391 At the species level, differences in test morphology related to topography  
392 were significant for *Adercotryma glomeratum*, *R.* sp. 14 and *R.* sp. 21. In the case of  
393 *A. glomeratum* it was the combined effect of all 31 morphometric parameters that  
394 drove the difference. Specimens from the plain sites were finely agglutinated with

395 smooth and circular tests (Pl. 3, figs 1–2), similar to previous descriptions of this  
396 species (see Taxonomic Appendix), while hill specimens had a rougher surface (Pl.  
397 3, figs 3–4), a reflection of the coarser sediment fractions present in these settings.  
398 However, their general shape and outline remained recognisable in both cases and  
399 there was little doubt that they represented the same morphospecies. Specimens of  
400 *R. sp. 14* from the plain sites had low convexity and sphericity values consistent with  
401 their elongate tests (Pl. 2, fig. 1), while hill specimens commonly agglutinated large,  
402 rounded to sub-rounded grains, resulting in a more spherical test (Pl. 2, fig. 2).  
403 Similarly, specimens of *R. sp. 21* from the hills had lower maximum to minimum  
404 diameter ratios and higher sphericity than those from the plain. In this case, the  
405 incorporation of large particles obscured the basic test morphology, which often  
406 made identification more difficult (Pl. 2, figs 5–6.). We conclude that the  
407 incorporation of large grains tends to make elongate tests more spherical in shape  
408 (*R. sp. 14*, *R. sp. 21*), and make spherical tests less spherical (*A. glomeratum*).

409

#### 410 **4.4 Evidence of mineral selectivity**

411 ESEM-EDS analyses revealed significant overlaps in the elemental composition of  
412 agglutinated tests in relation to topographic setting. In contrast, the elemental  
413 composition of hill and plain sediments was different when using the MDS x-ordinate  
414 as a variable in a Student's t-test ( $p < 0.01$ ), most likely as result of the different  
415 environmental conditions prevalent in the two settings. For example, Turnewitsch *et*  
416 *al.* (2004) demonstrated hydrodynamic near-bottom sorting and selective  
417 deposition/erosion of particles of differing sizes and chemical composition on a large  
418 abyssal hill in the PAP-SO area. They concluded that area of increasing near-bottom  
419 flow (erosiveness) tended to have higher concentrations of large and heavy particles

420 (e.g. Zircon) than more quiescent sites. In our case, sediments from the hill sites are  
421 subject to winnowing processes that preferentially remove the finer particles (e.g.  
422 coccoliths, small quartz grains) from the hilltops and deposit them on the adjacent  
423 plain, leaving the hill sediments enriched with coarser material (e.g. dead planktonic  
424 foraminifera tests, pebble to cobble-sized ice-rafted stones). It is likely that such  
425 processes are responsible for the distinct elemental profiles in the two settings.

426         The clear differences in the elemental composition of the tests and the  
427 sediments (Fig. 3a) indicated that foraminiferans favour certain minerals. The  
428 sediment at the PAP-SO is a carbonate ooze and as a result, many species found in  
429 the same area have tests made of planktonic foraminifera shells, including species  
430 of *Reophax* and *Lagenammina* (Gooday et al., 2010, fig. 13A–B; fig. 14F). Thus the  
431 presence of agglutinated taxa with tests made exclusively of mineral grains indicates  
432 a certain degree of mineral selection. Based on EDS spectra, the foraminifera in our  
433 samples had tests composed largely of quartz grains, regardless of species or site of  
434 origin. Quartz has been identified as the main test component of agglutinated  
435 foraminifera in marginal marine settings (Allen *et al.*, 1999), the deep sea (Gooday,  
436 1986; Gooday & Claugher, 1989) and in ancient marine environments (Mancin,  
437 2001; Mancin *et al.*, 2012), including carbonate-dominated habitats where this  
438 mineral occurred only in negligible amounts (Jørgensen, 1977). The selection of a  
439 quartz as a test component must confer certain benefits for the agglutinated  
440 foraminifera. Quartz is a stable mineral, with a consistent density and high resistance  
441 to weathering (Drever, 1985). Its use could help to make agglutinated foraminiferal  
442 tests more robust (Mancin *et al.*, 2012), at least in the case of species with firmly  
443 cemented tests like *Adercotryma glomeratum*, *Cribrostomoides* spp. or  
444 *Ammobaculites agglutinans* (Schröder, 1988), all of which are present in our study

445 sites (Pl. 1, figs. 3–10; Pl. 3, figs.1–4). Benthic foraminifera (mainly calcareous) living  
446 in physically stressed coastal habitats have stronger tests than those from nearby  
447 more tranquil localities (Wetmore, 1987). It is possible that a similar relationship  
448 applies in hydrographically different deep-sea settings.

449

#### 450 **4.5 Paleooceanographic significance**

451 The rich fossil record of benthic foraminifera makes them ideal tools for  
452 paleoenvironmental reconstructions. Traditionally, there has been an emphasis on  
453 calcareous taxa due to their high fossilization potential (Gooday, 2003; Rohling &  
454 Cooke, 2003; Jorissen *et al.*, 2007). However, agglutinated foraminifera are  
455 sometimes a major component of fossil assemblages, especially in “flysch-type” or  
456 “high latitude slope deep-water agglutinated foraminifera” faunas (Brouwer, 1965;  
457 Gradstein & Berggren, 1981; Kaminski *et al.*, 1989a; Kaminski *et al.*, 1989b;  
458 Kaminski *et al.*, 1995; Nagy *et al.*, 1997; Peryt *et al.*, 1997; Nagy *et al.*, 2000; Peryt  
459 *et al.*, 2004; Reolid *et al.*, 2008; Reolid *et al.*, 2010; Setoyama *et al.*, 2011;  
460 Waskowska, 2011) and can convey important palaeoecological information (Jones &  
461 Charnock, 1985; Alve & Murray, 1999; Murray & Alve, 1999b, a; Murray & Alve,  
462 2001; Murray *et al.*, 2011). Careful analysis has shown that modern agglutinated  
463 assemblages provide effective proxies for inferring past ecological conditions  
464 (Kaminski & Schröder, 1987 ; Nagy, 1992; Jones, 1999; Preece *et al.*, 1999; Jones  
465 *et al.*, 2005; Kender *et al.*, 2008). Additional studies on modern agglutinated  
466 foraminiferal faunas will help to refine their use in paleoceanography. The present  
467 results indicate that some abyssal NE Atlantic species are fairly consistent in terms  
468 of their test elemental composition, and hence presumably their selection of  
469 particular minerals (predominately quartz). Although we found no statistical support

470 for selection of particles in terms of size, there were differences in terms of the visual  
471 appearance and overall morphometry of the tests, which were more irregularly  
472 shaped ('lumpier') at the hill sites, H4 in particular. These characteristics  
473 (incorporation of coarse particles, test morphometry) could provide evidence for the  
474 recognition of ancient abyssal hills environments, as well as other  
475 palaeoceanographic settings that were characterised by enhanced current flow  
476 (Kaminski, 1985; Kaminski & Schröder, 1987 ; Nagy *et al.*, 1997). Certain taxa are  
477 clearly better suited to this task than others. In accordance with our findings,  
478 *Adercotryma glomeratum*, *Cribrostomoides subglobosum* and species of the genus  
479 *Reophax* have been elsewhere reported to reflect the nature of the surrounding  
480 sediments (Schröder *et al.*, 1988). These taxa, which are an important component of  
481 modern foraminiferal assemblages in the PAP-SO area, could be potential indicators  
482 of ancient environments exposed to enhanced near-bottom flow.

483

#### 484 **ACKNOWLEDGEMENTS**

485 We thank the captain and the crew of the R.R.S. *James Cook* and the scientists  
486 participating in JC062 for their assistance with the field operations. In addition, we  
487 thank Dr. Guillame Mabilieu at SCIAM, Angers University, for kindly helping us with  
488 the SEM and ESEM-EDS analysis; and Professor Ian Croudace for helping us with  
489 WD-XRF analysis of the sediment samples; Dr Veerle A I Huvenne for assistance  
490 with the sediment grain size analysis. One of us (PVS) had funding from the  
491 Graduate School of Ocean and Earth Sciences, University of Southampton that  
492 made possible the three-month stay and work in the Laboratory of Recent and Fossil  
493 Bio-Indicators (BIAF) at the University of Angers. We would also like to acknowledge  
494 the financial contribution of the Cushman Foundation for Foraminiferal Research

495 through the Loeblich and Tappan Student Research Award, which was awarded to  
496 one of us (PVS). In addition, we thank Professor Frans Jorissen, director of BIAF, for  
497 kindly allowing PVS to use all facilities during those three months and the rest of the  
498 working group for making this three-month visit a most pleasant experience. This  
499 research contributes to the NERC-funded efforts of the Autonomous Ecological  
500 Survey of the Abyss project (AESAs; NE/H021787/1) and the Porcupine Abyssal  
501 Plain Sustained Observatory Programme.

502

503

504

505

506

507

508

509

510

511

512

513

514

515

516

517

518

519

520 **TAXONOMIC APPENDIX**

521 The following notes include all named species and all open nomenclature species.  
522 For named species, we give the author, the original generic designation, and  
523 references to representative illustrations. Open nomenclature species are briefly  
524 characterized and compared, where possible, to a published illustration.

525

526 *Adercotryma glomeratum* (Pl. 3, figs 1–4). The specimens included here are  
527 more or less rounded, almost circular in shape with four chambers in the final whorl.  
528 The almost circular shape is more pronounced in specimens from the abyssal plain  
529 than those from hill sites. In general, they closely resemble *A. glomeratum* (Brady,  
530 1878) as illustrated in Brönniman and Whittaker (1987, figs 4a–4e), Timm (1992, pl.  
531 4, fig. 1a), Hayward *et al.* (2010, pl. 2, fig. 20), as well as the oval-shaped  
532 morphotype of *A. glomeratum* illustrated in Gooday *et al.* (2010, fig. 15e).

533

534 *Ammobaculites agglutinans* (d'Orbigny, 1846) (Pl. 1, figs 7–8). Our  
535 specimens resemble those illustrated by Brady (1884, pl. 32, figs 19, 20, 24–26) as  
536 *Spirolina agglutinans* d'Orbigny 1846.

537

538 *Cribrostomoides subglobosum* (Cushman, 1910) (Pl. 1, figs 8, 9; Pl. 2, figs 7,  
539 8). Our specimens resemble those illustrated by Brady (1884, pl. 34, figs 8–10) as  
540 *Haplophragmium latidorsatus*. This well-known species is widely reported from  
541 different oceans (Gooday & Jorissen, 2012).

542

543 *Lagenammia* sp. 1 (Pl. 3, figs 5–12). We included here two similar  
544 morphotypes with tests composed of mineral grains. One morphotype (Pl. 3, figs 5–

545 8) has an oval-shaped chamber with a relatively narrow apertural neck and is  
546 probably conspecific with *Reophax* cf. *diffflugiformis* Brady 1879 of Timm (1992, pl. 1,  
547 fig. 13a, b), *Lagenammina diffflugiformis* of Schiebel (1992, pl. 8, fig. 9), *L.*  
548 *diffflugiformis* subsp. *arenulata* (Skinner, 1961) of Wollenburg (1992, pl. 2, fig. 3), as  
549 well as the 'morphotype resembling *L. diffflugiformis*' of Gooday *et al.* (2010, fig. 13c)  
550 from the PAP-SO central site. The other morphotype has a generally more elongate  
551 test with a relatively wider apertural neck (Pl. 3, figs 9–12) and resembles another of  
552 the *Lagenammina* species illustrated by Gooday *et al.* (2010, fig. 13f). The two forms  
553 could not be separated consistently, as in the case of specimens from the abyssal  
554 hills the shape of the test was partly or completely obscured by coarse mineral  
555 grains. Consequently, we regarded both morphotypes as being the same species.  
556 Length up to 650  $\mu\text{m}$ .

557

558 *Portatrochammina murrayi* Brönnimann and Zaninetti, 1984 (Pl. 1, figs 9–10).  
559 Our specimens illustrate those described in Brönnimann and Zaninetti, 1984 (Pl. 5,  
560 figs 7, 12–15), Gooday (1986, fig. 100, P) and Dorst & Schönfeld (2015, fig. 3a, b  
561 and fig. 4a, b). This species has a wide bathymetric range (Murray & Alve, 2011).

562

563 *Recurvoides* sp. 9 (Pl. 1, figs 1–2). Test sub-rounded, streptospirally coiled,  
564 occasionally incorporating large quartz grains. Last whorl consists of four to five  
565 chambers, which gradually increase in size. The aperture is small, simple, oval-  
566 shaped, and placed on the base of the final chamber. The wall is semi-opaque and  
567 its colour ranges from orange to yellowish brown. Length ~420  $\mu\text{m}$ .

568

569            *Reophax* sp. 9 (Pl. 1, figs 11–12). Test comprising two to three chambers, the  
570 final being substantially larger than the previous ones, and produced into a  
571 pronounced apertural neck. Wall is composed predominantly of mineral grains,  
572 which can be quite coarse in the case of specimens from abyssal hills. Length up to  
573 370  $\mu\text{m}$ .

574 *Remarks:* This species closely resembles *Reophax* sp. 112/113 of Gooday *et al.*  
575 (2010, Fig.14A) from the PAP-SO central site, *Reophax* sp. 14 of Cornelius &  
576 Gooday (2004, fig. 5c) and *Reophax* sp. PS2214-4 of Wollenburg & Mackensen  
577 (1998, Pl. 1, fig. 9).

578

579            *Reophax* dentaliniformis (Pl. 2, figs 1–2) Test long and slender, consisting of  
580 up to seven clearly defined chambers arranged along a straight or slightly curved  
581 axis. Chambers are clearly defined and become larger and more elongate distally,  
582 although never parallel-sided. Final chamber elongate with a short apertural neck.  
583 Test wall consists of mineral grains. Specimens from abyssal hills slightly deviate  
584 from the typical morphology of this species, due to the coarser material they  
585 agglutinate. Length up to 1400  $\mu\text{m}$ .

586 *Remarks:* This species closely resembles *Reophax dentaliniformis* of Brady (1884,  
587 pl. 30, figs 21, 22) in both the number and shape of the chambers. The final chamber  
588 lacks the almost cylindrical (parallel-sided) shape shown in Brady's Fig. 22, but the  
589 specimens on the type slide (ZF265) in the Natural History Museum, London, exhibit  
590 quite a lot of variability in this respect.

591

592            *Reophax* sp. 21 (Pl. 1, figs 3–6) Test rather elongate, occasionally slightly  
593 curved, comprising 4–6 more or less globular chambers, sometimes connected by

594 short necks. Chambers increase in size distally; final chamber with a relatively long  
595 apertural neck. Wall consists predominantly of mineral grains. This species is easy  
596 to recognise, despite the incorporation of large grains by specimens from the  
597 abyssal hills. Length up to 880  $\mu\text{m}$ .

598 *Remarks:* This species closely resembles *Reophax* sp. 116 of Gooday *et al.* (2010,  
599 Fig.14E) from the PAP-SO central site. In addition, it looks similar to *Reophax*  
600 *scorpiurus* in Schröder *et al.* (1988, pl. 5, figs. 1–2). However, given the range of test  
601 morphologies illustrated by Schröder (1986), it is possible that their concept of this  
602 species encompassed several genetically distinct entities.

603

604 *Reophax* sp. 28 (Pl. 1, figs 7–10) Test elongate, more or less straight,  
605 comprising four to five slim chambers, which gradually increase in size. The wall is  
606 largely made of mineral grains and it often incorporates a small number of long  
607 spicules. The final chamber is often particularly elongated and has a thin apertural  
608 neck. Length up to 830  $\mu\text{m}$ .

609 *Remarks:* This species closely resembles *Reophax* sp. 117 of Gooday *et al.* (2010,  
610 Fig. 14C) from the PAP-SO central site.

611

612

613

614

615

616

617

618

619 **Supplementary files**

620

621 **Appendix A**

622 List of species used for morphometric, particle size and elemental analyses.

623

624 **Appendix B**

625 Morphometric Data (31 morphometric parameter) for all 60 benthic foraminiferal tests used in this  
626 study (both for SEM and light images).

627

628 **Appendix C**

629 Elemental composition of the 56 benthic foraminiferal tests and 5 sediment samples used in this  
630 study.

631

632

633

634

635

636

637

638

639

640

641

642

643

644

645

646 **REFERENCES**

647

648       Abbireddy, C.O.R. & Clayton, C.R.I. 2009. A review of modern particle sizing methods.  
649 *Proceedings of the Institution of Civil Engineers-Geotechnical Engineering*, **162**(4): 193–201,  
650 doi: 10.1680/Geng.2009.162.4.193.

651       Adl, S.M., Simpson, A.G.B., Lane, C.E., Lukes, J., Bass, D., Bowser, S.S., Brown, M.W.,  
652 Burki, F., Dunthorn, M., Hampl, V., Heiss, A., Hoppenrath, M., Lara, E., le Gall, L., Lynn, D.H.,  
653 McManus, H., Mitchell, E.A.D., Mozley-Stanridge, S.E., Parfrey, L.W., Pawlowski, J., Rueckert,  
654 S., Shadwick, L., Schoch, C.L., Smirnov, A. & Spiegel, F.W. 2012. The Revised Classification of  
655 Eukaryotes. *Journal of Eukaryotic Microbiology*, **59**(5): 429–493, doi: 10.1111/J.1550-  
656 7408.2012.00644.X.

657       Allen, K., Roberts, S. & Murray, J.W. 1999. Marginal marine agglutinated foraminifera:  
658 affinities for mineral phases. *Journal of Micropalaeontology*, **18**: 183–191.

659       Aller, J.Y. 1989. Quantifying Sediment Disturbance by Bottom Currents and Its Effect on  
660 Benthic Communities in a Deep-Sea Western Boundary Zone. *Deep-Sea Research Part A–*  
661 *Oceanographic Research Papers*, **36**(6): 901–934, doi: 10.1016/0198-0149(89)90035-6.

662       Alve, E. & Murray, J.W. 1999. Marginal marine environments of the Skagerrak and  
663 Kattegat: a baseline study of living (stained) benthic foraminiferal ecology. *Palaeogeography*  
664 *Palaeoclimatology Palaeoecology*, **146**(1–4): 171–193, doi: 10.1016/S0031-0182(98)00131-  
665 X.

666       Baldrigi, E., Lavaleye, M., Aliani, S., Conversi, A. & Manini, E. 2014. Large Spatial Scale  
667 Variability in Bathyal Macrobenthos Abundance, Biomass, alpha- and beta-Diversity along  
668 the Mediterranean Continental Margin. *Plos One*, **9**(9): e107261, doi:  
669 10.1371/journal.pone.0107261.

670 Brady, H.B. 1884. Report on the Foraminifera dredged by H.M.S. Challenger during the  
671 years 1873–1876: Report of the Scientific Results of the Voyage of H.M.S. Challenger, 1873–  
672 1876. *Zoology*, **9**: 1–814.

673 Brönnimann, P. & Zaninetti, L. 1984. Agglutinated foraminifera mainly Trochamminacea  
674 from the Baia de Sepetiba, near Rio de Janeiro, Brazil. *Revue de Paléobiologie*, **3**: 63–115.

675 Brouwer, J. 1965. Agglutinated foraminiferal faunas from some turbiditic sequences I, II.  
676 *Proceedings Koninklijke Nederlandse Akademie van Wetenschappen series B*, **68**(5): 309–  
677 334.

678 Buchanan, J.B. & Hedley, R.H. 1960. A contribution to the biology of *Astrorhiza limicola*  
679 (Foraminifera). *Journal of the Marine Biological Association of the United Kingdom*, **39**(3):  
680 549–560.

681 Clark, M.R., Rowden, A.A., Schlacher, T., Williams, A., Consalvey, M., Stocks, K.I., Rogers,  
682 A.D., O'Hara, T.D., White, M., Shank, T.M. & Hall-Spencer, J.M. 2010. The Ecology of  
683 Seamounts: Structure, Function, and Human Impacts. *Annual Review of Marine Science*, **2**:  
684 253–278, doi: 10.1146/Annurev-Marine-120308-081109.

685 Clarke, K.R. & Gorley, R.N. 2006. *PRIMER v6: User Manual/Tutorial*. PRIMER-E, Plymouth,  
686 UK.

687 Cornelius, N. & Gooday, A.J. 2004. 'Live' (stained) deep-sea benthic foraminiferans in the  
688 western Weddell Sea: trends in abundance, diversity and taxonomic composition along a  
689 depth transect. *Deep-Sea Research Part II—Topical Studies in Oceanography*, **51**(14–16):  
690 1571–1602, doi: 10.1016/J.Dsr2.2004.06.024.

691 Dorst, S. & Schonfeld, J. 2015. Taxonomic Notes on Recent Benthic Foraminiferal Species  
692 of the Family Trochamminidae from the Celtic Sea. *Journal of Foraminiferal Research*, **45**(2):  
693 167-189.

694 Drever, J.I. 1985. *The Chemistry of Weathering*. New York, Reidel.

695 du Châtelet, E.A., Noiriél, C. & Delaine, M. 2013a. Three-Dimensional Morphological and  
696 Mineralogical Characterization of Testate Amebae. *Microscopy and Microanalysis*, **19**(6):  
697 1511–1522, doi: 10.1017/S1431927613013226.

698 du Châtelet, E.A., Frontalini, F., Guillot, F., Recourt, P. & Ventalon, S. 2013b. Surface  
699 analysis of agglutinated benthic foraminifera through ESEM-EDS and Raman analyses: An  
700 expeditious approach for tracing mineral diversity. *Marine Micropaleontology*, **105**: 18–29,  
701 doi: 10.1016/J.Marmicro.2013.10.001.

702 du Châtelet, E.A., Bout-Roumazielles, V., Coccioni, R., Frontalini, F., Guillot, F., Kaminski,  
703 M.A., Recourt, P., Riboulleau, A., Trentesaux, A., Tribovillard, N. & Ventalon, S. 2013c.  
704 Environmental control on shell structure and composition of agglutinated foraminifera  
705 along a proximal-distal transect in the Marmara Sea. *Marine Geology*, **335**: 114–128, doi:  
706 10.1016/J.Margeo.2012.10.013.

707 Durden, J.M., Bett, B.J., Jones, D.O.B., Huvenne, V.A.I. & Ruhl, H.A. 2015. Abyssal hills –  
708 hidden source of increased habitat heterogeneity, benthic megafaunal biomass and  
709 diversity in the deep sea *Progress in Oceanography*, doi:  
710 dx.doi.org/10.1016/j.pocean.2015.06.006.

711 Gage, E.J.D. & Bett, B.J. 2005. Deep-sea benthic sampling. *In*: Eleftheriou, A. & MacIntyre,  
712 A. (Eds) *Methods for the study of marine benthos*, 3rd ed. Blackwell Scientific, Oxford, UK,  
713 273–325.

714 Gage, J.D., Lamont, P.A. & Tyler, P.A. 1995. Deep-Sea Macrobenthic Communities at  
715 Contrasting Sites Off Portugal, Preliminary-Results. 1. Introduction and Diversity  
716 Comparisons. *Internationale Revue Der Gesamten Hydrobiologie*, **80**(2): 235–250, doi:  
717 10.1002/Iroh.19950800211.

718 Genin, A., Dayton, P.K., Lonsdale, P.F. & Spiess, F.N. 1986. Corals on Seamount Peaks  
719 Provide Evidence of Current Acceleration over Deep-Sea Topography. *Nature*, **322**(6074):  
720 59–61, doi: 10.1038/322059a0.

721 Goff, J.A. & Arbic, B.K. 2010. Global prediction of abyssal hill roughness statistics for use  
722 in ocean models from digital maps of paleo-spreading rate, paleo-ridge orientation, and  
723 sediment thickness. *Ocean Modelling*, **32**(1-2): 36–43, doi: 10.1016/J.Ocemod.2009.10.001.

724 Gooday, A.J. 1986. Meiofaunal foraminiferans from the bathyal Porcupine-Seabight  
725 (northeast Atlantic): size structure, standing stock, taxonomic composition, species-diversity  
726 and vertical-distribution in the sediment. *Deep Sea Research Part A–Oceanographic*  
727 *Research Papers*, **33**(10): 1345–1373, doi: 10.1016/0198-0149(86)90040-3.

728 Gooday, A.J. & Claugher, D. 1989. The Genus *Bathysiphon* (Protista, Foraminiferida) in  
729 the Northeast Atlantic - Sem Observations on the Wall Structure of 7 Species. *Journal of*  
730 *Natural History*, **23**(3): 591–611, doi: 10.1080/00222938900770331.

731 Gooday, A.J., Levin, L.A., Linke, P. & Heeger, T. 1992. The Role of Benthic Foraminifera in  
732 Deep-Sea Food Webs and Carbon Cycling. *Deep-Sea Food Chains and the Global Carbon*  
733 *Cycle*, **360**: 63–91.

734 Gooday, A.J. 2003. Benthic foraminifera (protista) as tools in deep-water  
735 palaeoceanography: Environmental influences on faunal characteristics. *Advances in Marine*  
736 *Biology*, **46**: 1–90, doi: 10.1016/S0065-2881(03)46002-1.

737 Gooday, A.J., Malzone, M.G., Bett, B.J. & Lamont, P.A. 2010. Decadal-scale changes in  
738 shallow-infaunal foraminiferal assemblages at the Porcupine Abyssal Plain, NE Atlantic.  
739 *Deep-Sea Research Part II–Topical Studies in Oceanography*, **57**: 1362–1382.

740 Gooday, A.J. & Jorissen, F.J. 2012. Benthic foraminiferal biogeography: controls on global  
741 distribution patterns in deep-water settings. *Annual Review of Marine Science*, **4**: 237–262,  
742 doi: 10.1146/Annurev-Marine-120709-142737.

743 Gradstein, F.M. & Berggren, W.A. 1981. Flysch-Type Agglutinated Foraminifera and the  
744 Maestrichtian to Paleogene History of the Labrador and North Seas. *Marine*  
745 *Micropaleontology*, **6**(3): 211–268.

746 Haake, F.-W. 1977. Living benthic Foraminifera in the Adriatic Sea: influence of water  
747 depth and sediment. *The Journal of Foraminiferal Research*, **7**(1): 62–75.

748 Hada, Y. 1957. Biology of the arenaceous foraminifera. *Journal of Science of the*  
749 *Suzugamine Women's College, Hiroshima, Japan*, **3**(B): 31–50.

750 Hartman, S.E., Lampitt, R.S., Larkin, K.E., Pagnani, M., Campbell, J., Gkritzalis, T., Jiang,  
751 Z.P., Pebody, C.A., Ruhl, H.A., Gooday, A.J., Bett, B.J., Billett, D.S.M., Provost, P., McLachlan,  
752 R., Turton, J.D. & Lankester, S. 2012. The Porcupine Abyssal Plain fixed-point sustained  
753 observatory (PAP-SO): variations and trends from the Northeast Atlantic fixed-point time-  
754 series. *Ices Journal of Marine Science*, **69**(5): 776–783, doi: 10.1093/icesjms/Fss077.

755 Hasemann, C. & Soltwedel, T. 2011. Small-Scale Heterogeneity in Deep-Sea Nematode  
756 Communities around Biogenic Structures. *Plos One*, **6**(12): e29152, doi:  
757 10.1371/journal.pone.0029152.

758 Hayward, B.W., Grenfell, H.R., Sabaa, A.T., Neil, H.L. & Buzas, M.A. 2010. *Recent New*  
759 *Zealand Deep-Water Benthic Foraminifera: Taxonomy, Ecologic Distribution, Biogeography,*  
760 *and Use in Paleoenvironmental Assessment*. Lower Hutt, New Zealand.

761 Heezen, B.C., Tharp, M. & Ewing, M. 1959. The floors of the oceans: I. The North Atlantic.  
762 *Geological Society of America Special Paper*, **65**: 1–126.

763 Heezen, B.C. & Holcombe, T.L. 1965. *Geographic distribution of bottom roughness in the*  
764 *North Atlantic*. Lamont Geological Observatory, Columbia University.

765 Jones, R.W. & Charnock, M.A. 1985. Morphogroups of agglutinated foraminifera. Their  
766 life positions and feeding habits and potential applicability in (paleo)ecological studies.  
767 *Revue de Paléobiologie*, **4**(2): 311–320.

768 Jones, R.W. 1999. Forties Field (North Sea) revisited: a demonstration of the value of  
769 historical micropalaeontological data. *Biostratigraphy in Production and Development*  
770 *Geology*, **152**: 185–200, doi: 10.1144/Gsl.Sp.1999.152.01.11.

771 Jones, R.W., Pickering, K.T., Boudagher-Fadel, M. & Matthews, S. 2005. Preliminary  
772 observations on the micropalaeontological characterization of submarine fan/channel sub-  
773 environments, Ainsa System, south-central Pyrenees, Spain. *Recent Developments in*  
774 *Applied Biostratigraphy*: 55–68.

775 Jørgensen, N.O. 1977. Wall structure of some arenaceous foraminifera from the  
776 Maastrichtian White Chalk (Denmark). *Journal of Foraminiferal Research*, **7**: 313–321.

777 Jorissen, F.J., Fontanier, C. & Thomas, E. 2007. Paleoceanographical proxies based on  
778 deep-sea benthic foraminiferal assemblage characteristics. *In*: Hillaire-Marcel, C. & de  
779 Vernal, A. (Eds) *Proxies in Late Cenozoic Paleoceanography: Part. 2: Biological tracers and*  
780 *biomarkers*, 263–326.

781 Kaminski, M.A. 1985. Evidence for Control of Abyssal Agglutinated Foraminiferal  
782 Community Structure by Substrate Disturbance - Results from the Hebble Area. *Marine*  
783 *Geology*, **66**(1–4): 113–131, doi: 10.1016/0025-3227(85)90025-8.

784 Kaminski, M.A. & Schröder, C.J. 1987 Environmental analysis of deep-sea agglutinated  
785 foraminifera: can we distinguish tranquil from disturbed environments? *Gulf Coast Section*

786 *SEPM Foundation Eighth Annual Research Conference. Selected papers and illustrated*  
787 *abstracts*, 90–93.

788 Kaminski, M.A., Gradstein, F.M. & Berggren, W.A. 1989a. Paleogene benthic foraminifer  
789 biostratigraphy and paleoecology at Site 647, southern Labrador Sea. *roceedings of the*  
790 *Ocean Drilling Program: Scientific Results*, **105**: 705–730.

791 Kaminski, M.A., Gradstein, F.M., Scott, D.B. & Mackinnon, K.D. 1989b. Neogene benthic  
792 foraminiferal stratigraphy and deep water history of Sites 645, 646, and 647, Baffin Bay and  
793 Labrador Sea. *Proceedings of the Ocean Drilling Program: Scientific Results*, **105**: 731–756.

794 Kaminski, M.A., Boersma, M., Tyszka, J. & Holbourn, A.E.L. 1995. Response of deep-water  
795 agglutinated foraminifera to dysoxic conditions in the California Borderland basins. *In*:  
796 Kaminski, M.A., Geroch, S. & Gasifski, M.A. (Eds) *Proceedings of the Fourth International*  
797 *Workshop on Agglutinated Foraminifera, Kraków, Poland, September 12-19, 1993*,  
798 Grzybowski Foundation Special Publication, **3**, 131–140.

799 Kender, S., Kaminski, M.A. & Jones, R.W. 2008. Early to middle Miocene foraminifera  
800 from the deep-sea Congo Fan, offshore Angola. *Micropaleontology*, **54**(6): 477–568.

801 Levin, L.A., Demaster, D.J., Mccann, L.D. & Thomas, C.L. 1986. Effects of Giant Protozoans  
802 (Class Xenophyophorea) on Deep-Seamount Benthos. *Marine Ecology Progress Series*, **29**(1):  
803 99–104, doi: 10.3354/Meps029099.

804 Levin, L.A. & Nittrouer, C.A. 1987. Textural characteristics of sediments on deep  
805 seamounts in the eastern Pacific Ocean between 10 N and 30 N. *Seamounts, Islands, and*  
806 *Atolls*, **43**: 187–203.

807 Levin, L.A. & Thomas, C.L. 1989. The influence of hydrodynamic regime on infaunal  
808 assemblages inhabiting carbonate sediments on central Pacific seamounts. *Deep-Sea*

809 *Research Part A–Oceanographic Research Papers*, **36**(12): 1897–1915, doi: 10.1016/0198-  
810 0149(89)90117-9.

811 Mancin, N. 2001. Agglutinated foraminifera from the Epiligurian succession (Middle  
812 Eocene/Lower Miocene, Northern Apennines, Italy): Scanning electron microscopic  
813 characterization and paleoenvironmental implications. *Journal of Foraminiferal Research*,  
814 **31**(4): 294–308, doi: 10.2113/0310294.

815 Mancin, N., Basso, E., Pirini, C. & Kaminski, M.A. 2012. Selective mineral composition,  
816 functional test morphology and paleoecology of the agglutinated foraminiferal genus  
817 *Colominella* Popescu, 1998 in the Mediterranean Pliocene (Liguria, Italy). *Geologica*  
818 *Carpathica*, **63**(6): 491–502, doi: 10.2478/V10096-012-0038-Y.

819 McCave, I.N., Manighetti, B. & Robinson, S.G. 1995. Sortable Silt and Fine Sediment Size  
820 Composition Slicing - Parameters for Paleocurrent Speed and Paleoceanography.  
821 *Paleoceanography*, **10**(3): 593–610, doi: 10.1029/94pa03039.

822 McCave, I.N. & Hall, I.R. 2006. Size sorting in marine muds: Processes, pitfalls, and  
823 prospects for paleoflow-speed proxies. *Geochemistry Geophysics Geosystems*, **7**, doi:  
824 10.1029/2006gc001284.

825 Murray, J.W. & Alve, E. 1999a. Natural dissolution of modern shallow water benthic  
826 foraminifera: taphonomic effects on the palaeoecological record. *Palaeogeography*  
827 *Palaeoclimatology Palaeoecology*, **146**(1–4): 195–209, doi: 10.1016/S0031-0182(98)00132-  
828 1.

829 Murray, J.W. & Alve, E. 1999b. Taphonomic experiments on marginal marine  
830 foraminiferal assemblages: how much ecological information is preserved?  
831 *Palaeogeography Palaeoclimatology Palaeoecology*, **149**(1–4): 183–197, doi:  
832 10.1016/S0031-0182(98)00200-4.

833 Murray, J.W. & Alve, E. 2001. Do calcareous dominated shelf foraminiferal assemblages  
834 leave worthwhile ecological information after their dissolution? . In: M. B. Hart, M. A.  
835 Kaminski & Smart, C.W. (Eds) *Proceedings of the Fifth International Workshop on*  
836 *Agglutinated Foraminifera, Plymouth, U.K., September 6–16, 1997*, Grzybowski Foundation  
837 Special Publication, **7**, 311–331.

838 Murray, J.W. & Alve, E. 2011. The distribution of agglutinated foraminifera in NW  
839 European seas: Baseline data for the interpretation of fossil assemblages. *Palaeontologia*  
840 *Electronica*, **14**(2): 1–41.

841 Murray, J.W., Alve, E. & Jones, B.W. 2011. A new look at modern agglutinated benthic  
842 foraminiferal morphogroups: their value in palaeoecological interpretation.  
843 *Palaeogeography Palaeoclimatology Palaeoecology*, **309**(3–4): 229–241, doi:  
844 10.1016/J.Palaeo.2011.06.006.

845 Nagy, J. 1992. Environmental Significance of Foraminiferal Morphogroups in Jurassic  
846 North-Sea Deltas. *Palaeogeography Palaeoclimatology Palaeoecology*, **95**(1–2): 111–134,  
847 doi: 10.1016/0031-0182(92)90168-5.

848 Nagy, J., Kaminski, M.A., Johnsen, K. & Mitlehner, A.G. 1997. Foraminiferal,  
849 palynomorph, and diatom biostratigraphy and paleoenvironments of the Tork Formation: a  
850 reference section for the Paleocene–Eocene transition in the western Barents Sea. In: Hass,  
851 H.C. & Kaminski, M.A. (Eds) *Contributions to the Micropaleontology and Paleooceanography*  
852 *of the Northern North Atlantic*. , Grzybowski Foundation Special Publication, **5**, 15–38.

853 Nagy, J., Kaminski, M.A., Kuhnt, W. & Bremer, M.A. 2000. Agglutinated foraminifera from  
854 neritic to bathyal facies in the Palaeogene of Spitsbergen and the Barents Sea In: Hart, M.B.,  
855 Kaminski, M.A. & Smart, C.W. (Eds) *Proceedings of the Fifth International Workshop on*  
856 *Agglutinated Foraminifera*. , Grzybowski Foundation Special Publication, **7**, 333–361.

857 Peryt, D., Lahodynsky, R. & Durakiewicz, T. 1997. Deep-water agglutinated foraminiferal  
858 changes and stable isotope profiles across the Cretaceous-Paleogene boundary in the  
859 Rotwandgraben section, Eastern Alps (Austria). *Palaeogeography Palaeoclimatology*  
860 *Palaeoecology*, **132**(1–4): 287–307, doi: 10.1016/S0031-0182(97)00056-4.

861 Peryt, D., Alegret, L. & Molina, E. 2004. Agglutinated foraminifers and their response to  
862 the Cretaceous/Paleogene (K/P) boundary event at Ain Settara, Tunisia. *In*: Bubík, M. &  
863 Kaminski, M.A. (Eds) *Proceedings of the Sixth International Workshop on Agglutinated*  
864 *Foraminifera*, Grzybowski Foundation Special Publication, **8**, 393–412.

865 Pitcher, T.J., Morato, T., Hart, P.J.B., Clark, M.R., Haggan, N. & Santos, R.S. 2007.  
866 *Seamounts: Ecology, Fisheries, and Conservation*. Blackwell, Oxford, UK.

867 Preece, R.C., Kaminski, M.A. & Dignes, T.W. 1999. Miocene benthonic foraminiferal  
868 morphogroups in an oxygen minimum zone, offshore Cabinda. *In*: Cameron, N.R., Bate, R.H.  
869 & Clure, V.S. (Eds) *The oil and gas habitats of the South Atlantic*, Geological Society Special  
870 Publication, **153**, 267–282.

871 Reolid, M., Rodriguez-Tovar, F.J., Nagy, J. & Oloriz, F. 2008. Benthic foraminiferal  
872 morphogroups of mid to outer shelf environments of the Late Jurassic (Prebetic Zone,  
873 southern Spain): Characterization of biofacies and environmental significance.  
874 *Palaeogeography Palaeoclimatology Palaeoecology*, **261**(3–4): 280–299, doi:  
875 10.1016/J.Palaeo.2008.01.021.

876 Reolid, M., Nagy, J. & Rodriguez-Tovar, F.J. 2010. Ecostratigraphic trends of Jurassic  
877 agglutinated foraminiferal assemblages as a response to sea-level changes in shelf deposits  
878 of Svalbard (Norway). *Palaeogeography Palaeoclimatology Palaeoecology*, **293**(1–2): 184–  
879 196, doi: 10.1016/J.Palaeo.2010.05.019.

880 Rex, M.A. & Etter, R.J. 2010. *Deep-sea biodiversity: pattern and scale*. MA: Harvard  
881 University Press, Cambridge.

882 Rohling, E.J. & Cooke, S. 2003. Stable oxygen and carbon isotopes in foraminiferal  
883 carbonate shells. *In: Gupta, B.K.S. (Ed) Modern foraminifera*. Springer Netherlands, 239–  
884 258.

885 Ruggiero, M.A., Gordon, D.P., Orrell, T.M., Bailly, N., Bourgoin, T., Brusca, R.C., Cavalier-  
886 Smith, T., Guiry, M.D. & Kirk, P.M. 2015. A Higher Level Classification of All Living Organisms.  
887 *Plos One*, **10**(4): 1–60, doi: 10.1371/journal.pone.0119248.

888 Ruhl, H. 2012. *RRS James Cook Cruise 62, 24 Jul-29 Aug 2011. Porcupine Abyssal Plain –*  
889 *sustained observatory research*. National Oceanography Centre, Southampton.

890 Schiebel, R. 1992. Rezente benthische Foraminiferen in Sedimenten des Schelfes un  
891 oberen Kontinentalhanges im Golf von Guinea (Westafrika). *Berichte–Reports, Geologisch-*  
892 *Päpöntologisches Institut Universität Kiel*, **51**: 1–179.

893 Schröder, C.J. 1986. Deep-water arenaceous foraminifera in the northwest Atlantic  
894 Ocean *Canadian Technical Report of Hydrography and Ocean Sciences*, **71**: 1–191.

895 Schröder, C.J. 1988. Subsurface preservation of agglutinated foraminifera in the  
896 Northwest Atlantic Ocean. *Abhandlungen der Geologischen Bundesanstalt*, **41**: 325–336.

897 Schröder, C.J., Scott, D.B., Medioli, F.S., Bernstein, B.B. & Hessler, R.R. 1988. Larger  
898 agglutinated Foraminifera: comparison of assemblages from central North Pacific and  
899 Western North Atlantic (Nares Abyssal Plain). *Journal of Foraminiferal Research*, **18**(1): 25–  
900 41.

901 Setoyama, E., Kaminski, M.A. & Tyszka, J. 2011. The Late Cretaceous-Early Paleocene  
902 palaeobathymetric trends in the southwestern Barents Sea - Palaeoenvironmental

903 implications of benthic foraminiferal assemblage analysis. *Palaeogeography*  
904 *Palaeoclimatology Palaeoecology*, **307**(1–4): 44–58, doi: 10.1016/J.Palaeo.2011.04.021.

905 Slama, D.C. 1954. Arenaceous tests in foraminifera: an experiment. *The*  
906 *Micropaleontologist*, **8**: 33–34.

907 Snelgrove, P.V.R. & Smith, C.R. 2002. A riot of species in an environmental calm: The  
908 paradox of the species-rich deep-sea floor. *Oceanography and Marine Biology*, **40**: 311–342.

909 Stuart, C.T., Arbizu, P.M., Smith, C.R., Molodtsova, T., Brandt, A., Etter, R.J., Escobar-  
910 Briones, E., Fabri, M.C. & Rex, M.A. 2008. CeDAMar global database of abyssal biological  
911 sampling. *Aquatic Biology*, **4**(2): 143–145, doi: 10.3354/Ab00097.

912 Thistle, D. 1983. The Stability Time Hypothesis as a Predictor of Diversity in Deep-Sea  
913 Soft-Bottom Communities - a Test. *Deep-Sea Research Part A–Oceanographic Research*  
914 *Papers*, **30**(3): 267–277, doi: 10.1016/0198-0149(83)90010-9.

915 Thistle, D. & Eckman, J.E. 1990. The Effect of a Biologically Produced Structure on the  
916 Benthic Copepods of a Deep-Sea Site. *Deep-Sea Research Part A–Oceanographic Research*  
917 *Papers*, **37**(4): 541–554, doi: 10.1016/0198-0149(90)90089-E.

918 Thomsen, E. & Rasmussen, T.L. 2008. Coccolith-agglutinating foraminifera from the early  
919 Cretaceous and how they constructed their tests. *Journal of Foraminiferal Research*, **38**(3):  
920 193–214, doi: 10.2113/Gsjfr.38.3.193.

921 Timm, S. 1992. Rezente Tiefsee-Benthosforaminiferen aus Oberflächen-sedimenten des  
922 Golfes von Guinea (Westafrika) - Taxonomie, Verbreitung, Ökologie und  
923 Korngrößenfraktionen. *Berichte–Reports, Geologisch-Palontologisches Institut und*  
924 *Christian-Albrechts-Universität Kiel*, **59**: 1–155.

925 Turnewitsch, R., Reys, J.L., Chapman, D.C., Thomson, J. & Lampitt, R.S. 2004. Evidence  
926 for a sedimentary fingerprint of an asymmetric flow field surrounding a short seamount.  
927 *Earth and Planetary Science Letters*, **222**(3–4): 1023–1036, doi: 10.1016/J.Epsl.2004.03.042.

928 Turnewitsch, R., Falahat, S., Nycander, J., Dale, A., Scott, R.B. & Furnival, D. 2013. Deep-  
929 sea fluid and sediment dynamics-Influence of hill- to seamount-scale seafloor topography.  
930 *Earth-Science Reviews*, **127**: 203–241, doi: 10.1016/J.Earscirev.2013.10.005.

931 Warren, R., VanDerWal, J., Price, J., Welbergen, J.A., Atkinson, I., Ramirez-Villegas, J.,  
932 Osborn, T.J., Jarvis, A., Shoo, L.P. & Williams, S.E. 2013. Quantifying the benefit of early  
933 climate change mitigation in avoiding biodiversity loss. *Nature Climate Change*, **3**: 678–682.

934 Waskowska, A. 2011. Response of Early Eocene deep-water benthic foraminifera to  
935 volcanic ash falls in the Polish Outer Carpathians: Palaeocological implications.  
936 *Palaeogeography Palaeoclimatology Palaeoecology*, **305**(1–4): 50–64, doi:  
937 10.1016/J.Palaeo.2011.02.012.

938 Watling, L., Guinotte, J., Clark, M.R. & Smith, C.R. 2013. A proposed biogeography of the  
939 deep ocean floor. *Progress in Oceanography*, **111**: 91–112.

940 Wells, P.E. 1985. Recent Agglutinated Benthonic Foraminifera (Suborder Textulariina) of  
941 Wellington Harbor, New-Zealand. *New Zealand Journal of Marine and Freshwater Research*,  
942 **19**(4): 575–599.

943 Wetmore, K.L. 1987. Correlations between Test Strength, Morphology and Habitat in  
944 Some Benthic Foraminifera from the Coast of Washington. *Journal of Foraminiferal*  
945 *Research*, **17**(1): 1–13.

946 Wollenburg, J.E. 1992. Zur Taxonomie von resented benthischen Foraminiferen aus dem  
947 Nansen Becken, Arktischer Ozean. *Berichte zur Polarforschung*, **112**: 1–137.

948 Wollenburg, J.E. & Mackensen, A. 1998. Living benthic foraminifers from the central  
949 Arctic Ocean: faunal composition, standing stock and diversity. *Marine Micropaleontology*,  
950 **34**(3): 153–185.

951 Yesson, C., Clark, M.R., Taylor, M.L. & Rogers, A.D. 2011. The global distribution of  
952 seamounts based on 30 arc seconds bathymetry data. *Deep-Sea Research Part I–*  
953 *Oceanographic Research Papers*, **58**(4): 442–453, doi: 10.1016/J.Dsr.2011.02.004.

954

955

956

957

958

959

960

961

962

963

964

965

966

967

968

969

970

971

972

973

974 **Fig. 1.** Bathymetric map of the PAP-SO area showing the positions of the four study sites, P3 and P4  
975 (abyssal plain sites), H1 and H4 (abyssal hill sites). Black triangles indicate the location of the core  
976 samples from which foraminiferal specimens were collected. Green circles and red squares indicate  
977 the location of the core samples that were used for estimating particle size distribution and elemental  
978 composition of the sediments, respectively. The inset indicates the general location of the Porcupine  
979 Abyssal Plain in the northeast Atlantic Ocean.

980

981 **Explanation of Plate 1.** Light and SEM photographs of some species used in this study along with  
982 the site of collection. **figs 1–2.** *Recurvoides* sp. 9 (H1). **figs 3–6.** *Cribrostomoides subglobosum*: **3–4**  
983 (P3); **5–6** (H4). **figs 7–8.** *Ammobaculites agglutinans* (H1). **figs 9–10.** *Portatrochammina murrayi*  
984 (H4). **figs 11–12.** *Reophax* sp. 9.

985

986 **Explanation of Plate 2.** Light and SEM photographs of *Reophax* spp. used in this study along with  
987 the site of collection. **figs 1–2.** *Reophax dentalinoformis*: **1**, (P4); **2**, (H4). **figs 3–6.** *Reophax* sp. 21:  
988 **3–4**, (P4); **5–6**, (H4). **figs 7–10.** *Reophax* sp. 28: **7–8**, (P4); **9–10**, (H1). Scale bars = 100  $\mu\text{m}$ .

989

990 **Explanation of Plate 3.** Light and SEM photographs of some species used in this study along with  
991 the site of collection. **figs 1–4.** *Adercotryma glomeratum*: **1–2**, (P4); **3–4**, (H4). **figs 5–10.**  
992 *Lagenammina* sp. 1: 1<sup>st</sup> morphotype, **5–6**, (P4), **7–8** (H4); 2<sup>nd</sup> morphotype, **9–10** (P4), **11–12** (H4).  
993 Scale bars = 100  $\mu\text{m}$ .

994

995 **Fig. 2. (a)** Mean particle size distribution (0–1 cm sediment horizon) of sediment samples from the  
996 four study sites. **(b)** MDS on the particle size distribution of 56 benthic foraminiferal tests and  
997 seventeen sediment samples from four sites. **(c)** Box-Whisker plots of the MDS x- and y-ordinate for  
998 the sediment samples and foraminiferal tests against topography. **(d)** Mean particle size distribution  
999 (0–1 cm sediment horizon) of the foraminiferal tests and sediment samples from the four study sites.

1000

1001 **Fig. 3. (a)** MDS on the elemental composition (13 common elements: 10 major, 3 trace) of 56 benthic  
1002 foraminiferal tests and five sediment samples from four sites. **(b)** MDS on the elemental composition

1003 (16 elements: 10 major, 6 trace) of the 56 benthic foraminiferal tests. **(c)** MDS on the elemental (32  
1004 elements: 11 major, 21 trace) composition of the five sediment samples.

1005

1006

1007

1008

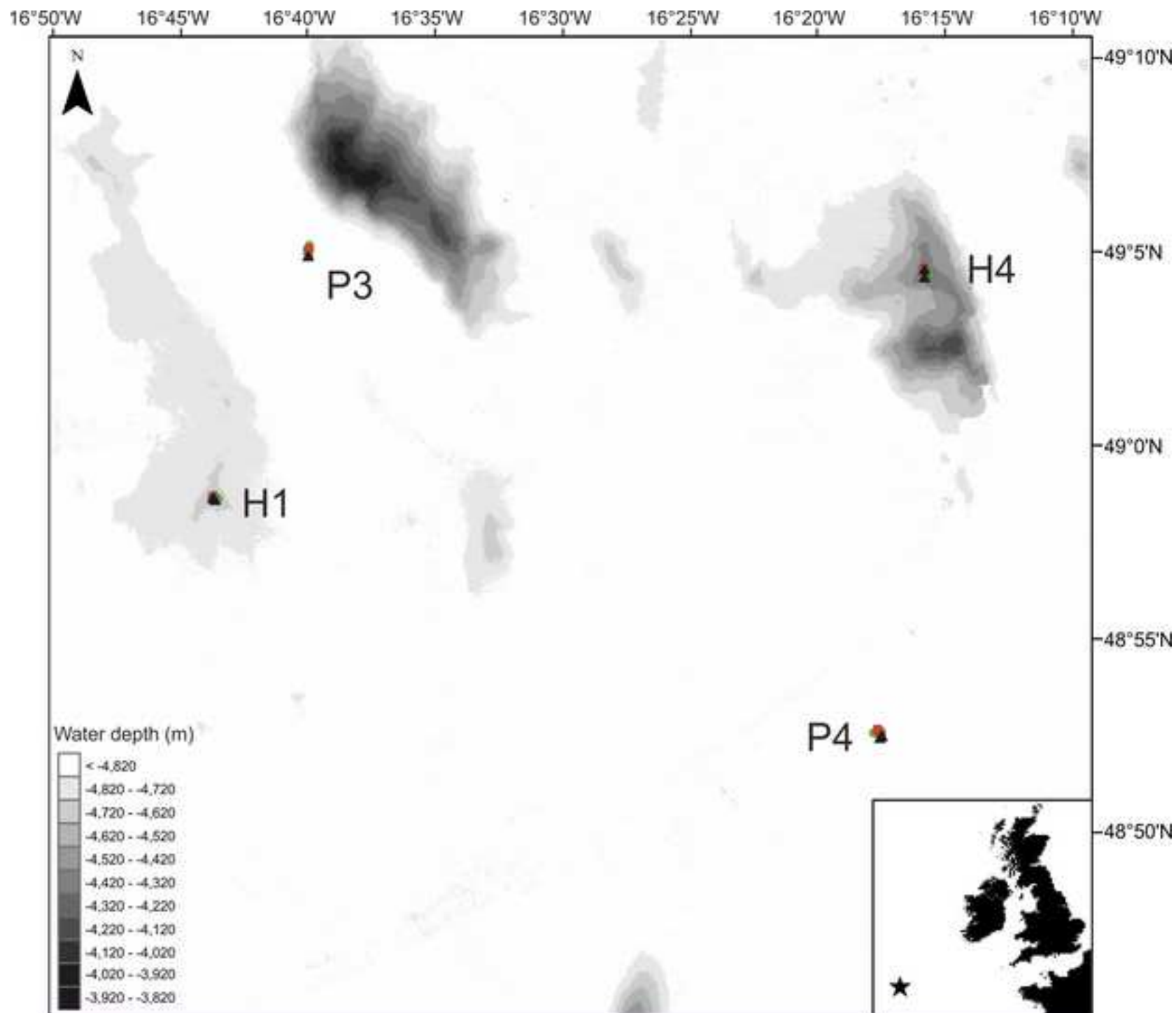
1009

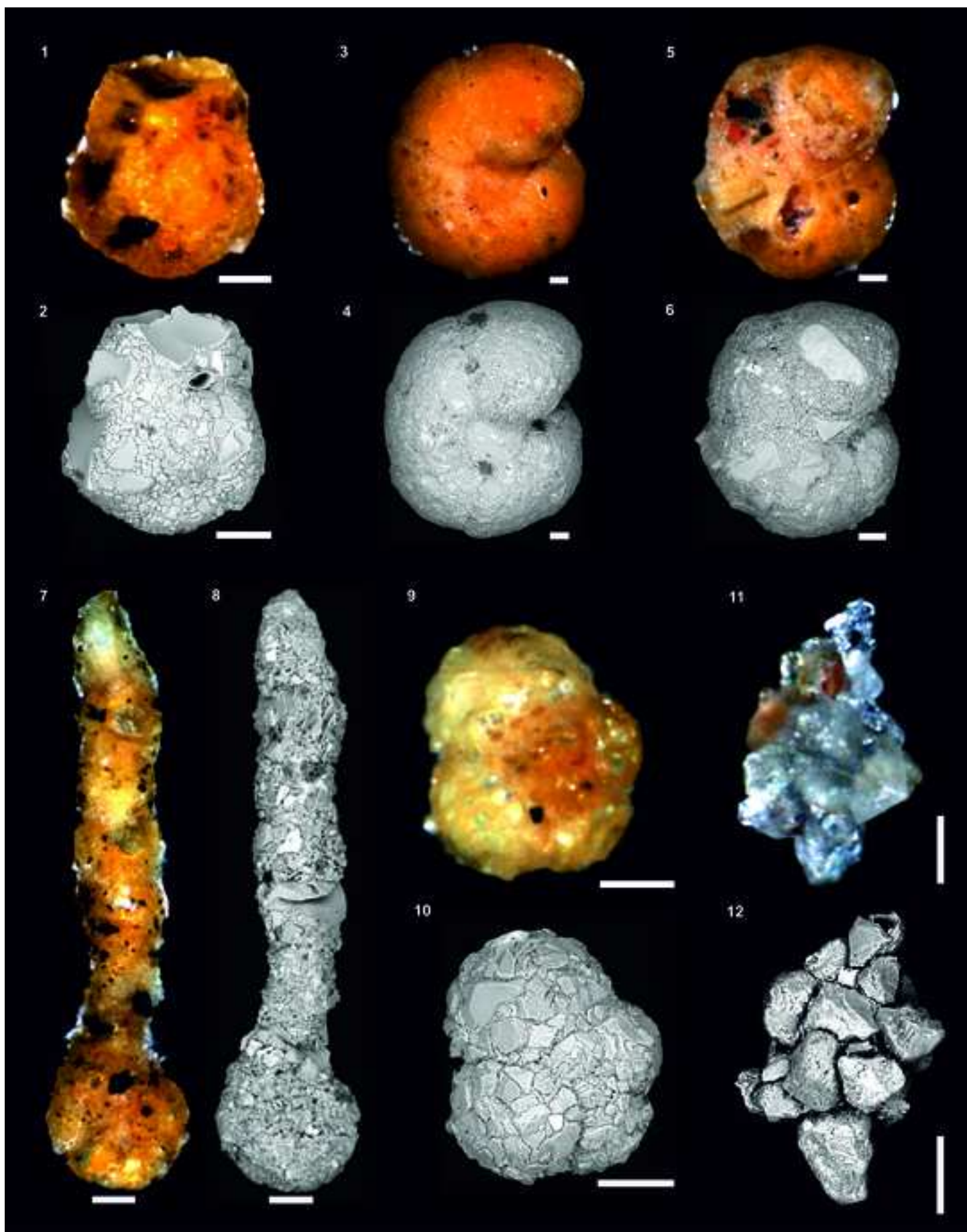
1010

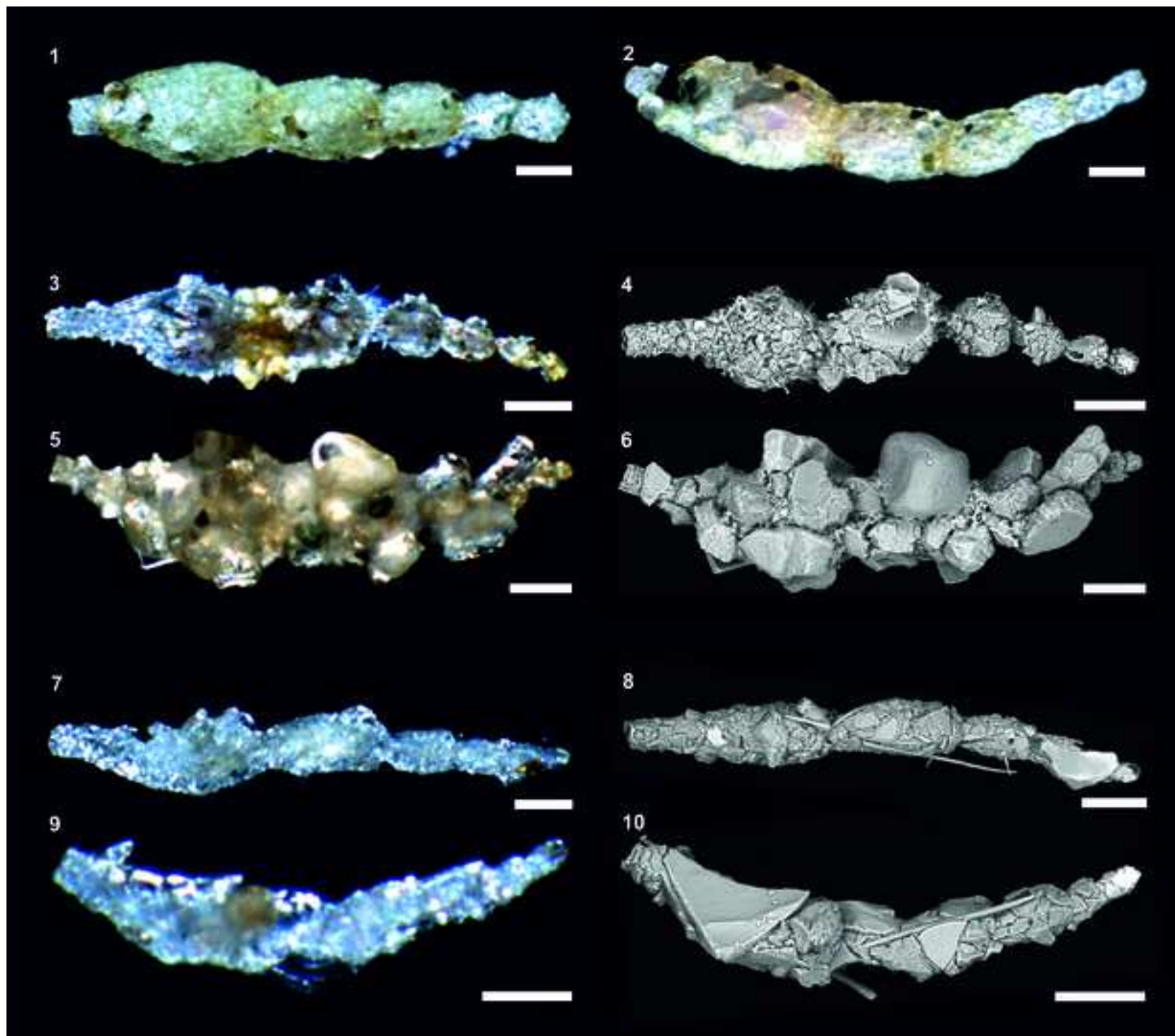
1011

1012

Figure 1  
[Click here to download high resolution image](#)







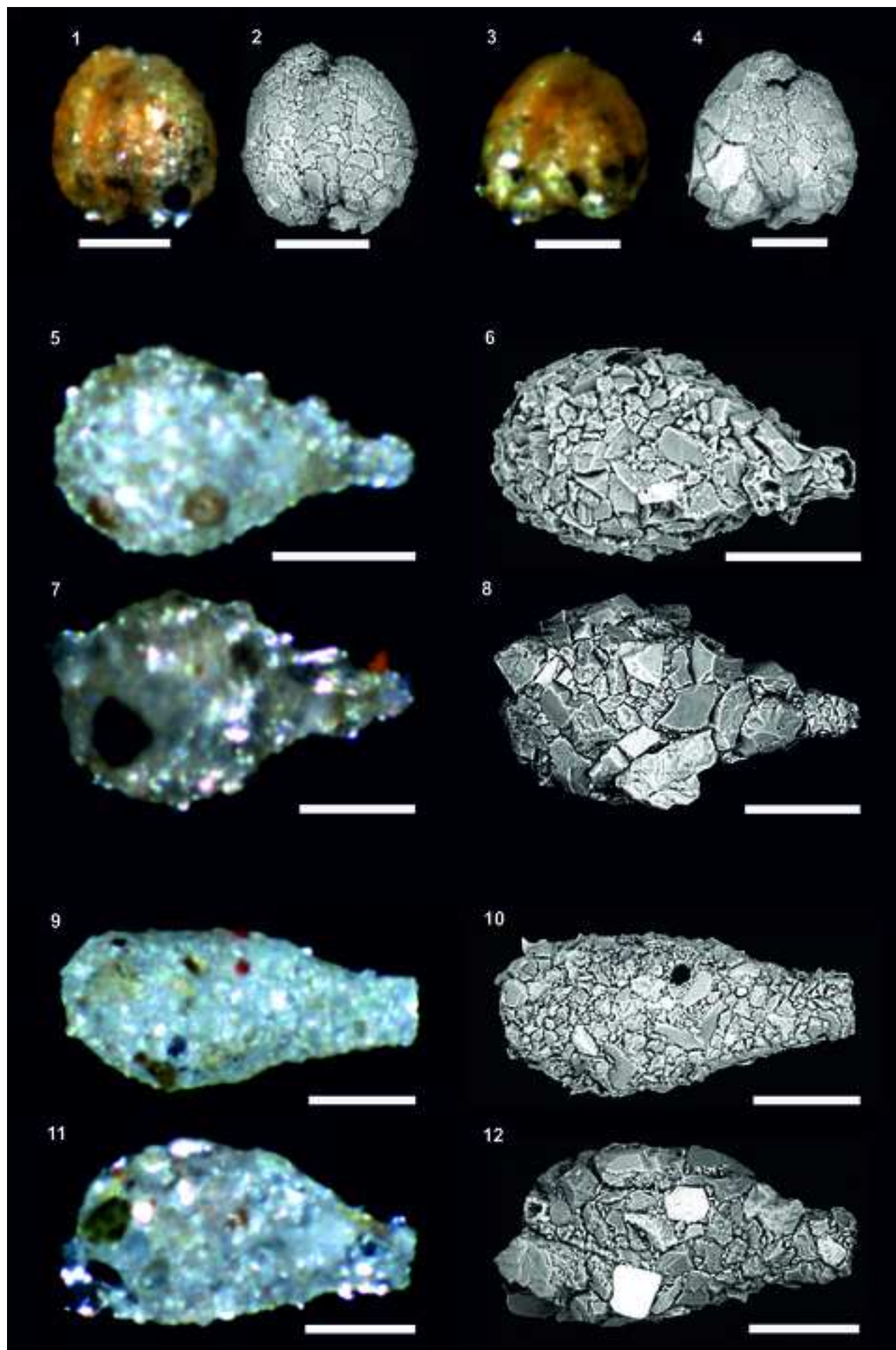


Figure 2  
[Click here to download high resolution image](#)

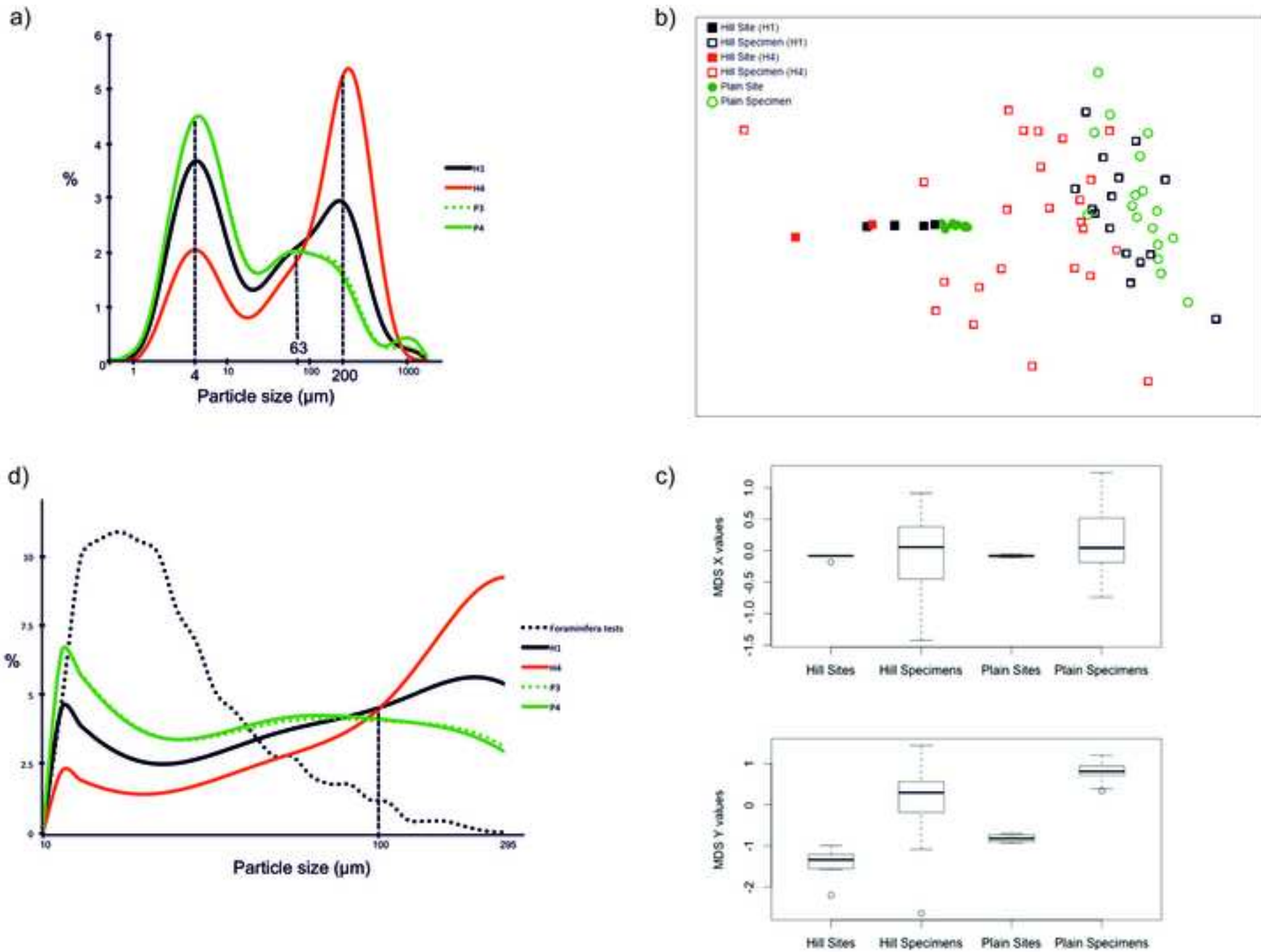
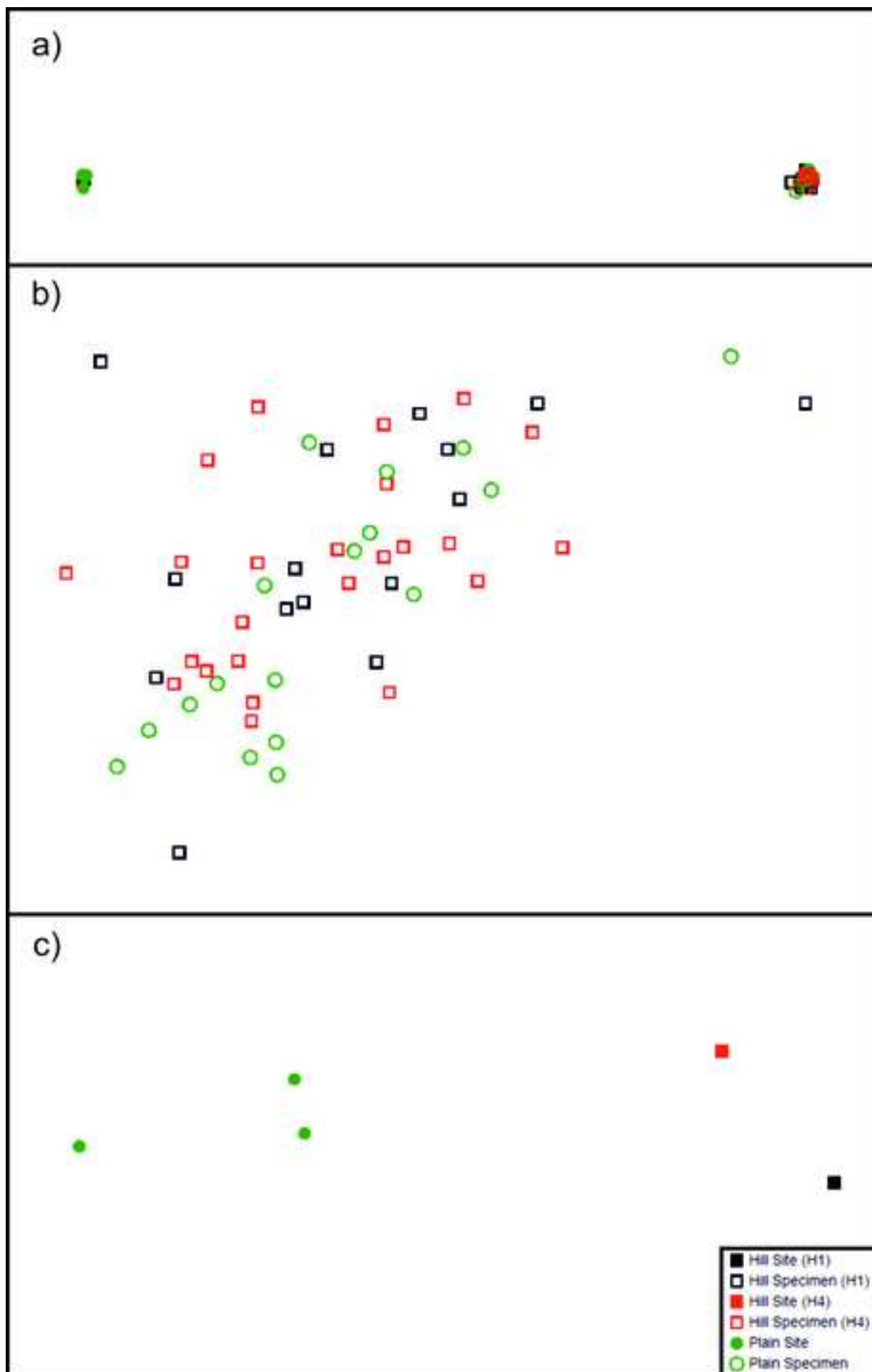


Figure 3  
[Click here to download high resolution image](#)



## Appendix A

[Click here to download Supplementary Data for online publication only: Appendix A.docx](#)

## Appendix B

[Click here to download Supplementary Data for online publication only: Appendix B.xlsx](#)

## Appendix C

[Click here to download Supplementary Data for online publication only: Appendix C.xlsx](#)